ALMA MATER STUDIORUM - UNIVERSITÀ DI BOLOGNA

SCUOLA DI INGEGNERIA E ARCHITETTURA

Dipartimento di Ingegneria civile, chimica, ambientale e dei Materiali
DICAM

CIVIL ENGINEERING

TESI DI LAUREA

in
Structural Safety

THE EFFECT OF THE DUCTILITY ON THE COLLAPSE LOADS: THE FAILURE OF A STEEL ROOF

CANDIDATO:

Lorenzo Carlet

RELATORE:

Chiar.mo Prof. Tomaso Trombetti

CORRELATORE:
Prof. Stefano Silvestri

Anno Accademico 2013/2014

Sessione III

ABSTRACT

Nella pratica ingegneristica l'attività progettuale è basata sull'utilizzo di modelli il cui scopo è dare una rappresentazione sintetica ma allo stesso tempo vicina alla realtà fisica. Tali modelli in genere non tengono mai conto di imperfezioni che immancabilmente si presentano nel corso della realizzazione e della vita di utilizzo delle strutture, imperfezioni che possono implicare, per strutture iperstatiche, degli stati coattivi che si traducono in sollecitazioni addizionali, ma che per la loro natura aleatoria sono difficili da individuare e modellizzare. Di fronte alla complessità del problema il progettista dimentica consapevolmente tali situazioni, non solo per semplificare l'approccio progettuale ma soprattutto delegando il riassorbimento di tali sollecitazioni addizionali alla duttilità dei materiali e degli elementi strutturali.

In questo senso si sviluppa lo scopo della tesi: investigare la relazione che gli stati coattivi dovuti a imperfezioni di realizzazione, effetti termici o cedimenti vincolari hanno con il carico ultimo sopportabile da strutture dotate di una certa duttilità.

In particolare utilizzando calcoli a mano e programmi di calcolo delle strutture il moltiplicatore critico dei carichi λcr, che rappresenta il carico d collasso, è calcolato nel caso di diverse strutture di crescente complessità, caratterizzate da diversi livelli di imperfezioni iniziali ξ e di duttilità μ:

$$\lambda_{CR} = \lambda_{CR}(\xi\ ;\ \mu)$$

I risultati verranno dunque raccolti e confrontati per verificare come, per le strutture indagate, la duttilità giochi effettivamente un ruolo cruciale nell'insensibilità del carico di collasso agli stati coattivi iniziali.

SUMMARY

1. INTRODUCTION 6
1.1 BACKGROUND 6
1.2 AIM OF THE THESIS 6
1.3 STRUCTURE OF THE THESIS 6
2. ULTIMATE LOAD THEORY 8
2.1 HISTORY OF ULTIMATE LOAD METHOD 8
2.1.1 FIRST PUBLICATIONS 8
2.1.2 CONTROVERSIES 9
2.1.3 THEORY DEVELOPEMENT & CONSENT 10
3. THEORY OF PLASTICITY 12
3.1 INTRODUCTION 12
3.1.1 THE CONCEPT OF DUCTILITY 12
3.1.2 THE EXAMPLE OF THE THREE RODS – THE BENFIT OF STRUCTURAL DUCTILIY 15
3.1.3 RECTANGULAR CROSS SECTION UNDER BENDING 18
3.1.4 PROPORTIONAL LOADING – THE LOAD MULTIPLIER 20
3.1.5 CONCENTRATED PLASTICITY - THE PLASTIC HINGE 20
3.2 INCREMENTAL PLASTIC ANALYSIS 21
3.2.1 INCREMENTAL ANALYSIS METHOD 21
3.3 LIMIT PLASTIC ANALYS 22
3.3.1 THEOREMS OF LIMIT ANALYSIS 22
3.3.2 DISTRIBUTED LOADS 24
3.3.1 RUPTURE ANALYSIS – NON-INFINITELY DUCTILE STRUCUTRES 24
3.3.2 DEPENDENCE OF λ_{CR} ON COERCIVE STATES 24
3.4 RELIABILITY OF STRUCTURES 25
3.4.1 SERIES SYSTEMS 25
3.4.2 PARALLEL SYSTEMS 26
3.4.3 DUCTILE BEHAVIOUR & STRUCTURAL SAFETY 27
4. THE ANALYTICAL STUDY 30
4.1 LIMIT PLASTIC ANALYSY 30
4.1.1 FIRST EXAMPLE – CONCENTRATED LOAD 30
4.1.2 SECOND EXAMPLE – DISTRIBUTED LOAD 31
4.2 INCREMENTAL PLASTIC ANALYSIS 32

4.2.1 FIRST EXAMPLE – CONCENTRATED LOAD 32
4.2.2 SECOND EXAMPLE – DISTRIBUTED LOAD 36
4.3 SOFTWARE IMPLEMENTATION 41
4.3.1 STRUCTURAL DESCRIPTION 41
4.3.2 FIRST EXAMPLE – CONCENTRATED FORCE 43
4.3.3 SECOND EXAMPLE – DISTRIBUTED LOAD 45
4.4 BRITTLE BEHAVIOUR & CONCLUSIONS 48
5. CONCRETE FRAME 50
5.1 STRUCTURE DESCRIPTION 50
5.1.1 GEOMETRICL DESCRIPTION 50
5.1.2 MATERIAL PROPERTIES 50
5.1.3 CROSS-SECION PROPERTIES 51
5.2 ACTIONS 53
5.2.1 VERTICAL LOADS 53
5.2.2 SETTLEMENT CONFIGURATIONS 53
5.3 STATIC PLASTIC ANALYSIS (VERTICAL PUSH-OVER) 55
5.3.1 CROSS-SECTION MODELS 55
5.3.2 “WEAK BEAM” STRUCTURE 57
5.3.3 “WEAK COLUMN” STRUCTURE 58
5.4 CONCLUSIONS 60
6. PORTOMAGGIORE STUDY CASE 62
6.1 INTRODUCTION 62
6.1.1 DESCRIPTION OF THE STRUCTURE 62
6.1.2 TRUSS SYSTEM DESCRIPTION 65
6.2 ACTIONS 70
6.2.1 PERMANENT LOADS 70
6.2.2 VARIABLE LOADS 70
6.3 STRUCTURAL ANALYSYS 71
6.3.1 LINEAR ELASTIC ANALYSYS 71
6.3.2 BUCKLING ANALYSIS & VERIFICATIONS 73
6.4 STATIC PLASTIC ANALYSIS (PUSH-OVER) 74
6.4.1 CROSS-SECTION MODELS 74
6.4.2 “STOCKY-ELEMENTS” STRUCTURE 77
6.4.3 “SLENDER-ELEMENTS” STRUCTURE 78
6.4.4 “SLENDER ELEMENTS WITH CONNECTORS” STRUCTURE 79

6.5 CONCLUSIONS 80
7. CONCLUSIONS 82
8. BIBLIOGRAPHY 83

1. INTRODUCTION

1.1 BACKGROUND

The usual design approach of structures leans on the assumption of applying the theories of structural mechanics to models that are thought to be the best representation of the real behaviour of the structural system but intrinsically imply its simplification. One of the most important, but sometimes under-estimated, is to not take into account for coercive states given by constraint displacements, components imperfections, thermal effects or construction processes in structural redundant structures. The verification of such situations and their impact on structural safety are usually complex to be identified and quantified. This simplification approach may seem superficial and lay on the unsafe side, but actually leans on the idea that local damage of structures do not influence the ultimate loading capacity of a structure given its ductility. The plasticity of the material and the ductility of components are thought to be the properties that allow the structure to adapt to the coercive states and overcome the presence of elevated local stresses.

The topic of the influence of accidental coercive states on ultimate loading capacity is however not completely developed and entrusted to ductility

1.2 AIM OF THE THESIS

The aim of this thesis is to investigate the interaction between the collapse load and imperfections causing initial coercive states at different levels of ductility. Different types of structures and materials will be examined and subjected to different types of initial distortions, the collapse load will be then computed as a function of not only the element resistance but also of the level of initial distortion and the element ductility.

1.3 STRUCTURE OF THE THESIS

The thesis is composed of six chapters:

1. the introduction;

2. the history of ultimate load theory and plasticity, where the main steps, authors and publications that brought to the final definition of the theory will be reported;

3. the description of basic concepts of the theory of plasticity, such as different definitions of ductility, the analytical tools to perform the incremental or the limit plastic analysis, the impact of plastic behaviour on structural safety.

4. the analytical study of one single beam fixed at the ends, where the previously described concepts are applied in some simple hand-made calculations. A simple software analysis is performed in order to get the hang of the software and compare the numerical results with the expected ones

5. the ultimate load of a multi-storey reinforce concrete planar frame, where three levels of ductility (infinitely ductile, real ductility and brittle) are defined in order to understand the collapse load relation with the initial distortion given by the settlement of the supports;

6. the real case of a collapsed steel roof under snow loads, where non-linear analysis are performed on different structural models, trying in understand and to represent the real behaviour of the structure and the lacks related with its unexpected collapse.

2. ULTIMATE LOAD THEORY

2.1 HISTORY OF ULTIMATE LOAD METHOD

Already from the last decades of 19th century structural engineers working with steel praised the "ingenuity" or the "self-help" of their plastic and ductile material when the expected results coming from linear elastic structural investigations did not reflect adequately the real load-bearing capacity.

In the following years a large number of researchers started to investigate this phenomenon, in order to quantify the strength reserves and to expose to criticism the linear-elastic stress-strain relation, known as Hooke's law, as far as it was no longer able to represent the real behaviour of structures subjected to limit load-bearing conditions. In the following paragraphs the terms "ultimate load method" and "plastic hinge method" will be used as synonyms.

2.1.1 FIRST PUBLICATIONS

In 1914 the Hungarian engineer Gàbor Kazinski experienced the first investigation approaches. He led experimental measurements of the ultimate distributed load *w* applied to a steel beam, fixed at both ends, with an double-T cross-section, encased in concrete, with free span L of 6,00 meters [Kazinski, 1914]. Kazinski concluded that the failure mode to be reached is the alignment of three plastic sections (plastic hinges), in a beam with two degrees of static indeterminacy. The resisting bending moment to be guaranteed is therefore no longer $wL^2/12$ but can be lower, with the value $wL^2/16$.

The economic design of steel structures that was involved in the previous statements became clear in the 1920s in Germany, Austria and Czechoslovakia and later in Great Britain and in the Soviet Union. The steel designers and producers gave a large impulse to the research on these topics, and many publications appeared in those years: Josef Fritsche, Karl Girkman, Martin Grüning and especially Maier-Leibnitz.

Hermann Maier-Leibnitz clarified the already known "ingenuity" or ductility of steel structures carrying out experiments on the load-bearing capacity of simply-supported beams and continuous beams, in 1928 he summarized his work on beams with two equal spans and illustrated how the critical design moment is not the central support negative moment but rather the positive span moment. At the second A.I.P.C. congress (Assoc. Intern. Ponts & Charp.) held in Berlin in 1936, Maier-Leibnitz reported his results on continuous steel beams showing the significant insensitivity of the load bearing capacity of such structures to relative displacements imposed to its supports, i.e. to conditions that would largely affect the results of a linear-elastic analysis.

Josef Fritsche in 1930 investigated the clumped beam, the two-spans and three-spans beams with the method of plastic hinges and stated that "*As the examples up to now show, calculating the load-carrying capacity is quite simple and avoids the – often tedious – calculation of the statically indeterminate variables, although knowledge of the purely elastic solution [...] is very helpful*."

Already in 1932, Karl Girkmann was able to define a comprehensively formulated plastic design method, based on the works of the previously described authors, resting on several hypothesis like the demand for a positive dissipation work, the assurance against local failure or local buckling or the proper design of connections in order to obtain dissipation in the members.

2.1.2 CONTROVERSIES

The previously described development of the plastic hinge method, and especially the branch of limit analysis caused strong reactions in a part of the academic world that criticized the excessive simplicity of such a method applied to statically-redundant structures.

In 1935 Fritz Stüssi & Curt Fritz Kollbrunner formulated the "paradox of plastic hinge method".

It is given a continuous beam on four supports, symmetric with respect to the middle point, where a concentrated force P is applied. The two lateral span are long l_1 while the central span is long l. The load P is increased until failure of the structure. The plastic limit state of such a structure is reached with the presence of three plastic hinges (two on the supports and one in the middle of the central span) that change the system with two degrees of redundancy into a simple kinematically determinate structure. In this case the ultimate load given by a limit analysis is $F_u = 8\,{}^{M_{pl}}/_{l}$ where l is the length of the central span and M_p is the plastic bending moment given by the section.

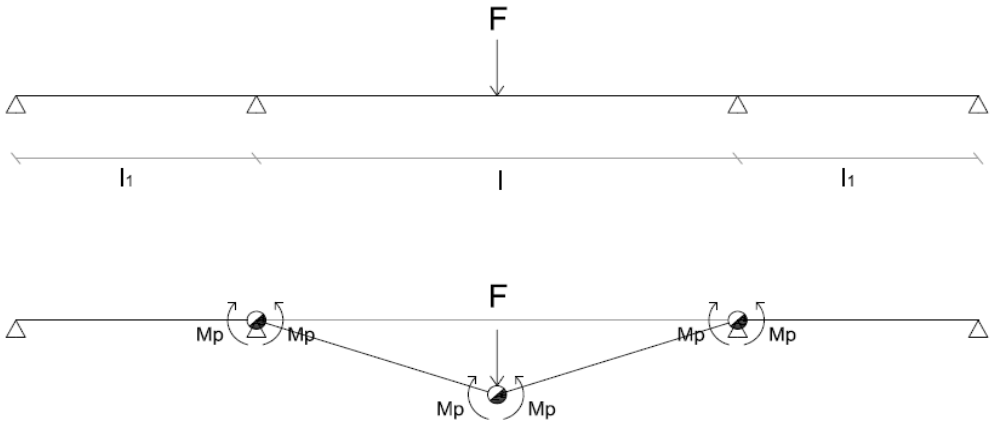

Figure 1 - paradox of plastic hinge method

By varying the length of the lateral spans l_1, different limit cases can be obtained:

when $l_1 \to 0$ the continuous beam tends to become a single beam of length l , clumped at the both ends, with an ultimate load of $F_u = 8\,{}^{M_{pl}}/_{l}$.

If $l_1 \to \infty$, the continuous beam tends to become a simple-supported beam of length l, which has a different ultimate load of $F_u = 4\,{}^{M_{pl}}/_{l}$.

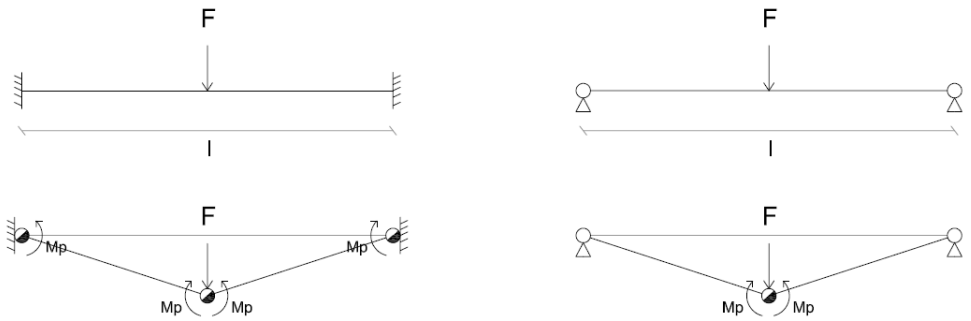

Figure 2 – limit cases

This paradox states that the ultimate load value depends on the relative stiffness of the members, and not only on the plastic moment magnitude. In fact, Kazinczy recognised this paradox already in 1931 and drew attention on the fact that the deflection of the beam in the case of $l_1 \to \infty$ "*reaches an unacceptable magnitude*".

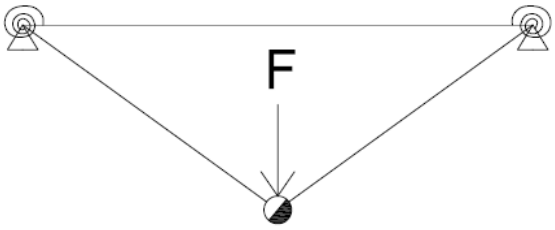

Figure 3 – actual behaviour

2.1.3 THEORY DEVELOPEMENT & CONSENT

The final contribution to the wide-spread use of the ultimate load theory was given by the so called "Anglo-American school of ultimate load" , developed by two professors, John Fleetwood Baker and William Prager, respectively from Cambridge and Brown Universities in the 1950s. They coordinated an intense research programme, together with several exchange programmes that led to a final rigorous formulation of plastic theory for steel frames. In 1956

Jacques Heyman, together with J.F. Baker and M.R. Horne published the first book on plastic theory for structural steelwork: "*The steel skeleton, Vol.2 : Plastic behaviour and design*" [Baker et al., 1956].This publication summarized all the work carried on by several teams in Cambridge in the previous ten years and was the first established mention to fundamental theorems of ultimate load theory together with the description of practical applications. It is to be reported that the fundamental theorems had been verified by the Soviet researcher Aleksei Aleksandrovich Gvozdev in 1936, but were unfortunately unknown to the West given that they were published only in Russian and only available through the Moscow Academy of Sciences.

Theory of plasticity experienced its consolidation in the 1970s and 1980s, when several manuals were published, which led to the widespread application of the theory. Later it was realised that the principles applied to steelwork were valid also for any ductile material and construction technique.

3. THEORY OF PLASTICITY

3.1 INTRODUCTION

The aim of the following chapter is to recall some basic concepts that will enable the reader to understand all the following computations and results. All the computations and the analytical methods will be founded by the following hypothesis:

- slender elements, with a compact and rigid cross-section (Eulero-Bernoulli beam);
- bilateral stress-strain diagram σ-ε, i.e. an elastic-perfectly plastic material;
- small displacement theory;
- flexural behaviour of plastic zones summarized and located in pointwise elements called "plastic hinges".

3.1.1 THE CONCEPT OF DUCTILITY

In the following lines, the concept of **ductility** will be introduced, with some practical examples in order to understand its effect on structures.

MATERIAL DUCTILITY

The ductility is the ability of a material to deform under stresses and in particular, in an elastic-perfectly plastic material to maintain the yielding stress f_y level until rupture ($\varepsilon=\varepsilon_u$). In Figure 4 the bilateral stress-strain diagram of an elastic-perfectly plastic material is represented:

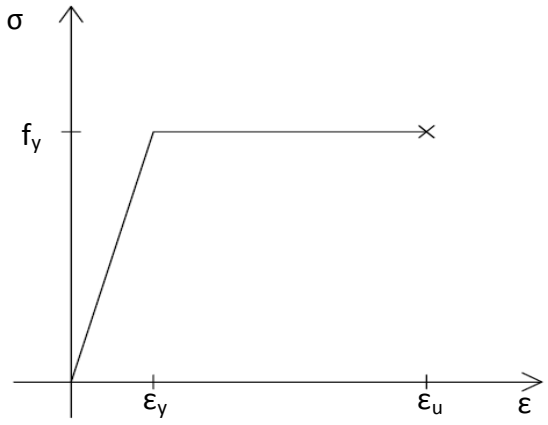

Figure 4 – elastic-perfectly plastic σ-ε diagram

The material ductility in such conditions is defined as:

$$\mu_{mat} = \frac{\varepsilon_u}{\varepsilon_y}$$

CROSS-SECTIONAL DUCTILITY

The idea of material ductility can be transposed also to the moment-curvature diagram, i.e. to a cross-sectional level. In the Figure 5 the tri-linear moment-curvature diagram (M-χ) of a general reinforced concrete section is depicted.

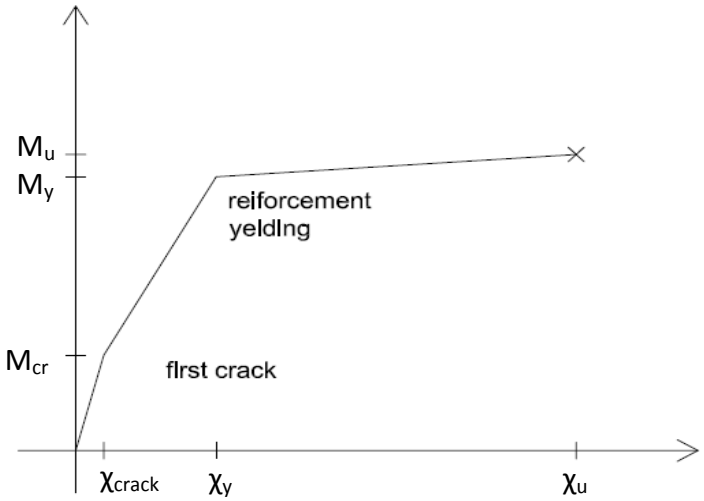

Figure 5 – trilinear M-χ diagram

The cross-sectional flexural ductility is the ability of a given cross-section to sustain a bending moment $M \geq M_y$ also after the yielding of its components, in this case:

$$\mu_{sec} = \frac{\chi_u}{\chi_y}$$

This feature of a given cross-section is not only given by the ductility of materials inserted in the cross-section but also of its geometry, so it is a synthetic parameter given by the ratio of the ultimate curvature at rupture and the curvature that involves the firs yielding of a component. Further features about the cross-section behaviour in elastic-plastic analysis will be reported in paragraph 3.1.3.

STRUCTURAL DUCTILITY

A further generalization of the concept of ductility is the structural ductility. A simple example follows: a cantilever vertical element is subjected to a horizontal force F, the top displacement u is monitored. The cross-section is meant to have an elastic-perfectly plastic behaviour, i.e. a bilinear moment-curvature diagram. The force-displacement diagram is depicted as follows:

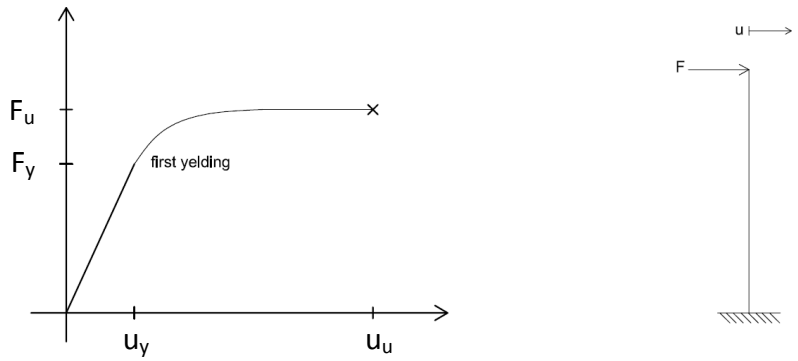

Figure 6 – structural force-displacement curve

Until the yielding of the first cross-section at the bottom of the column the structure behaviour is linear elastic. For further increments of the force F an increasing number of cross-sections is yielding, while the stiffness of the structure decreases (i.e. the increases of the top displacement u get larger for decreasing increments of force F) until the reaching of the ultimate curvature χ_u in the bottom cross-section that takes to failure the structure.

The structural ductility is thus given by the ratio between ultimate displacement u_u and yielding displacement u_y:

$$\mu_{str} = \frac{u_u}{u_y}$$

For more complex structural systems this ability of the structure to sustain loads also after yielding of its components is not only given by the material ductility and the cross-sectional ductility of its elements, but depends also on the geometrical arrangement of its components, their relative stiffness and resistance and the effectiveness of their connections. The structural ductility μ_{str} is thus a concise parameter to describe all the effectiveness of the previously mentioned features of a structure until its collapse.

3.1.2 THE EXAMPLE OF THE THREE RODS – THE BENFIT OF STRUCTURAL DUCTILIY

A classic example of the theory of plasticity is the case of three rods supporting a rigid body subjected to an increasing force F. The system depicted in Figure 7 – three rods example and its deformed confguration is symmetric, the central rod has a length l_1 and a cross-sectional area A, while the lateral rods have a length equal to l_2 and a cross-sectional area of A/2.

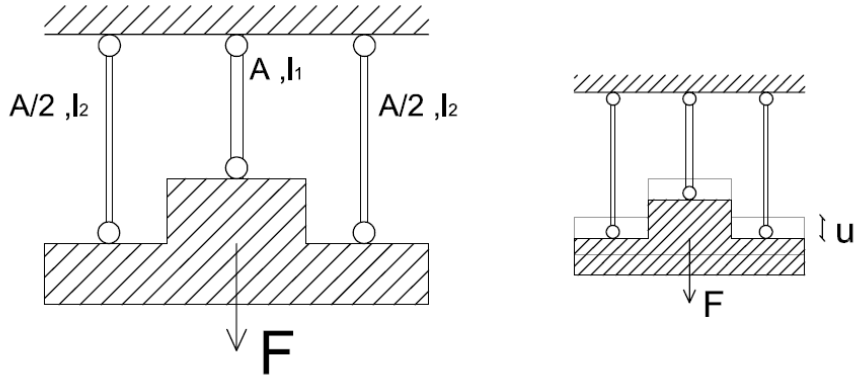

Figure 7 – three rods example and its deformed confguration

The rigid body subjected to the vertical force F moves downwards thus the three rods elongate of the same quantity in order to attain compatibility. The forces in the first elastic phase are thus distributed among the components proportionally to their relative stiffness:

- $F_1 = F_{tot}\,\frac{l_2}{l_1+l_2} \;\rightarrow\; \sigma_1 = \frac{F_{tot}}{A}\,\frac{l_2}{l_1+l_2}$ for the central rod;
- $F_2 = \frac{F_{tot}}{2}\,\frac{l_1}{l_1+l_2} \;\rightarrow\; \sigma_2 = \frac{F_{tot}}{A}\,\frac{l_1}{l_1+l_2}$ for the lateral rods.

In a first case the rods are thought to be made with a brittle material (i.e. $\mu_{mat} = \frac{\varepsilon_u}{\varepsilon_y} = 1$).

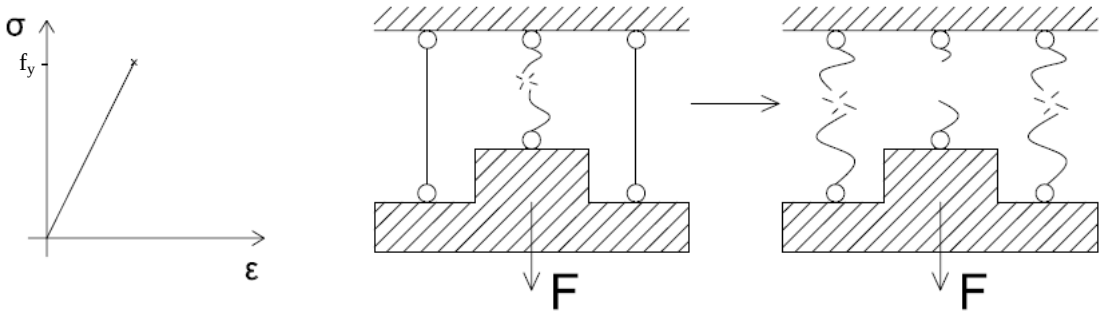

Figure 8 - brittle behaviour

When the central rod (the stiffer one) reaches the maximum capacity ($\sigma_1 = f_y$) it collapses because all its fibres reach simultaneously the maximum stress, the force is then transferred to

the only lateral rods that cannot support this abrupt increase of applied forces and immediately collapse. This failure mechanism, peculiar of brittle systems, is called progressive collapse. The force that takes to the maximum stress f_y the central rod is:

$$F_{tot,e} = F_{tot,u} = f_y A \left(1 + \frac{l_1}{l_2}\right)$$

In the second case the rods section are made of a material with the same stiffness and maximum stress f_y but with a remarkable material ductility $\mu_{mat} = \frac{\varepsilon_u}{\varepsilon_y} \gg 1$.

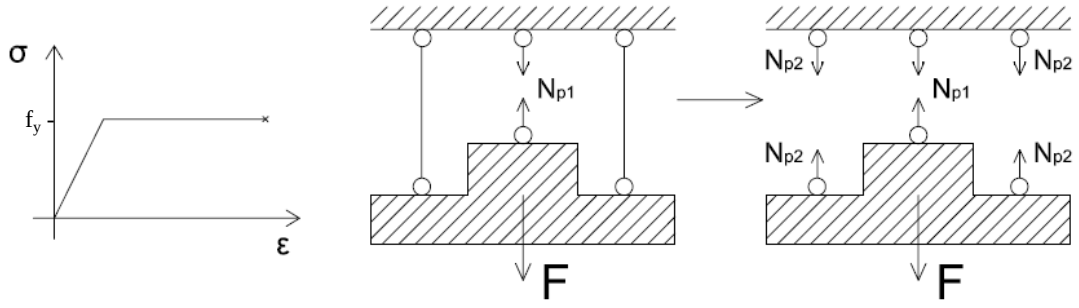

Figure 9 - ductile behaviour

In this second case, when the central rod reaches its maximum capacity ($\sigma_1 = f_y$), with the same external force $F_{tot,e} = f_y A \left(1 + \frac{l_1}{l_2}\right)$, it does not fail but it exerts its plastic force $N_{p,1} = A\, f_y$ for further downwards displacements that correspond to increments of the applied external force, until also the lateral rods yield. The ultimate condition of the structure is given by the three plastic forces ($N_{p,i=}A_i f_y$) applied to the rigid body. The external load in this condition is:

$$F_{tot,u} = F_{tot,p} = f_y A + 2\, \left(f_y \frac{A}{2}\right) = 2\, f_y A$$

The increase in the maximum external force is sensible and it is:

$$\frac{\Delta F_{tot}}{F_{tot,e}} = \frac{2 - \left(1 + \frac{l_1}{l_2}\right)}{\left(1 + \frac{l_1}{l_2}\right)}$$

at the limit $l_2 \gg l_1$ the increase is of 100% and it is given by the only increase in the material ductility, while the cross-section dimensions and maximum yielding stress remain constant. Moreover as previously reported about the structural ductility, the benefit of ductility, i.e. the increments of maximum external force and ultimate displacements, is not only function of the material ductility but also of geometrical arrangement of the structure (ratio l_1/l_2) . The structural behaviour is summarized in the following graph:

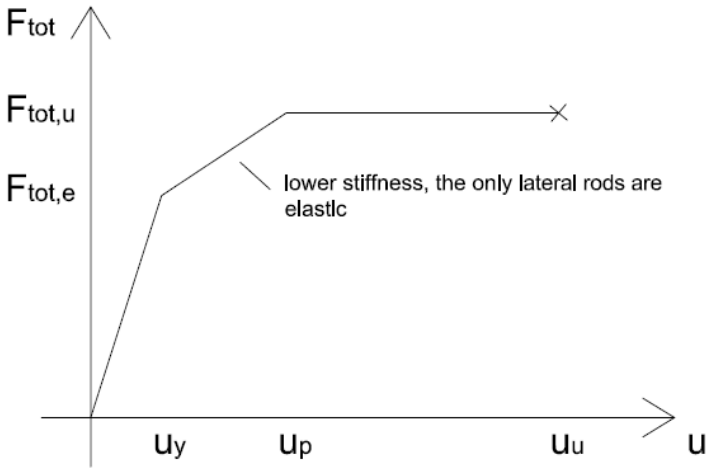

Figure 10 - force-displacement diagram

It is possible to notice how the stiffness of the structure decreases after the yielding of the first rod because the only stiffness is given by the only lateral rods that are still elastic. The ultimate displacement depends on the only ultimate strain of the material, but the force applied cannot exceed the value $F_{tot,u} = 2\, f_y A$.

3.1.3 RECTANGULAR CROSS SECTION UNDER BENDING

A very simple and effective tool in the plastic structural analysis is the concept of plastic hinge. In order to define it, the behaviour of a general cross-section subjected to bending moment is described in the following paragraph. It has to be reported that several yielding criteria $f(\sigma_x, \dots, \tau_{yz}) = k$ may be used in order to confront the presence of shear and normal stresses to the yielding stress. In the following paragraph the most simple framework of a cross-section with plastic behaviour will be applied, i.e. shear stresses will be neglected and the only axial state of stress will be taken into account.

Given a rectangular cross-section with a width equal to b and depth equal to h, the external bending moment will increase until a certain plastic flow will appear. The cross section is made of an elastic-perfectly plastic material with a strongly ductile behaviour ($\mu_{mat} = \frac{\varepsilon_u}{\varepsilon_y} \gg 1$).

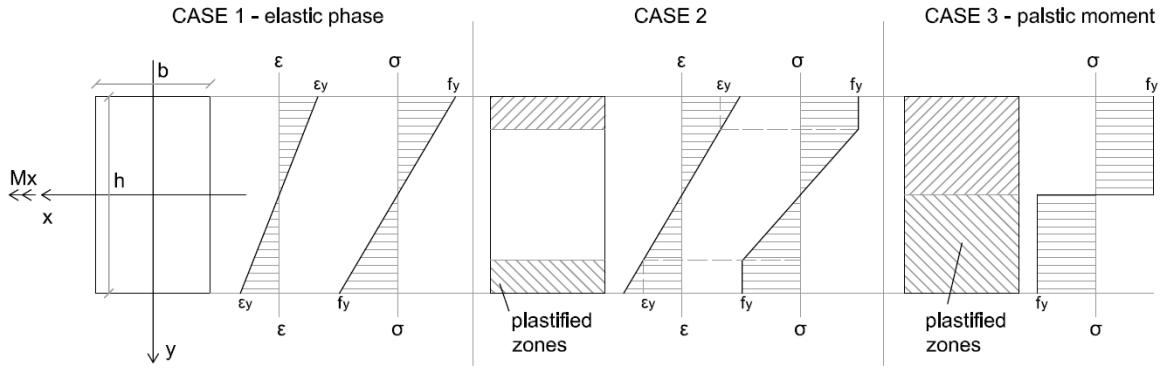

Figure 11- cross-sectional loading stages

The elastic limit of the cross-section is obtained when the most stressed fibre reaches the yielding condition (case 1):

$$\sigma = \frac{M_{ext}}{J}\frac{h}{2} = \frac{M_{ext}}{bh^2}6 = f_y$$

And the elastic bending moment is thus defined as:

$$M_{el} = W_e\, f_y = \frac{bh^2}{6}\, f_y$$

Where W_e is called elastic section modulus.

When the rod was considered all its fibres reached simultaneously the yielding condition, on the contrary the plastic behaviour of the rectangular cross-section starts from its edges while the internal fibres have still an elastic behaviour. Further increments of the external bending moment an increasing number of fibres undergo plastic strains (case 2). If the material composing the cross-section is thought to be infinitely ductile and the curvature χ tends to

infinite the cross-section exhibits half of its fibres yielded in tension and half in compression (case 3). In order to obtain rotation equilibrium in this case the external bending moment is equal to:

$$M_{ext} = M_p = \frac{bh}{2} f_y \frac{h}{2} = \frac{bh^2}{4} f_y = W_p f_y$$

Where M_p stands for plastic bending moment, and describes the limit condition $\chi \to \infty$. Wp is the plastic section modulus.

As mentioned in the previous paragraph the plastic benefit to the cross section takes to an increment in the maximum applied bending moment from the elastic to the plastic one, is not given by an increment in strength of the material but by the only presence of ductility.

The plastic benefit depends on the section geometry and in the case of a rectangular cross-section is given by:

$$\frac{M_p}{M_e} = \frac{W_p f_y}{W_e f_y} = \frac{6}{bh^2} \frac{bh^2}{4} \frac{f_y}{f_y} = \frac{3}{2}$$

The plastic benefit can vary a lot depending on the cross-section. In fig.edgg three different moment-curvature diagrams are depicted. the three cross-section have the same value of elastic bending moment M_e, but different plastic benefits depending on their shape, the rectangular one has a factor $\frac{W_p}{W_e}$ equal to 1,5 while the lumped-masses cross-section has no plastic benefit thus $\frac{W_p}{W_e} = 1$. Between these two "limit cases" rests a typical double-T shaped cross-section for which average values for the plastic benefit $\frac{W_p}{W_e}$ are 1,1 or 1,2.

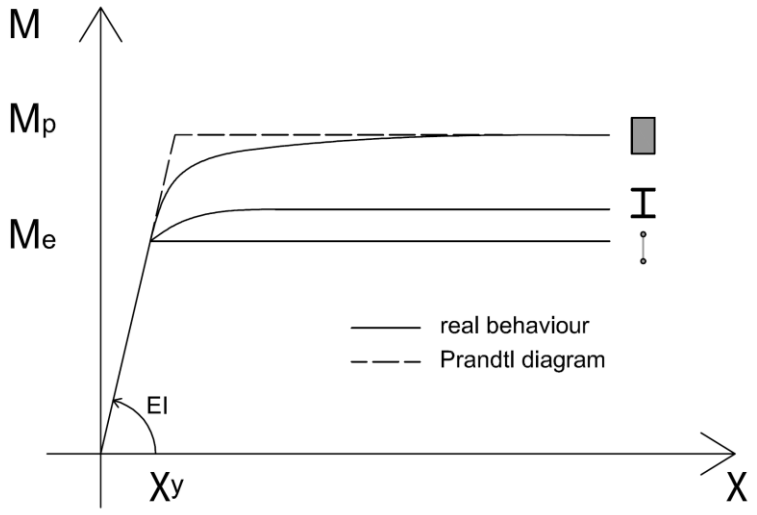

Figure 12 - M-χ diagram for different cross-sectional shapes

The first linear branch lasts until the elastic bending moment M_e is applied, for further increments an increasing number of fibres undergo plastic strains and the cross-sectional stiffness decreases, tending to zero while approaching the horizontal asymptote of M_p. The "speed" of convergence towards the value of M_p depends again on the geometry of the section.

A valid simplification of the cross-sectional plastic behaviour under bending is given by the bilinear Prandtl diagram, depicted inFigure 12. Even if this simplified bilinear moment-curvature diagram detaches from the real behaviour of the cross-section, the error is negligible. Moreover such M-χ diagram becomes a very strong tool for plastic analysis.

3.1.4 PROPORTIONAL LOADING – THE LOAD MULTIPLIER

In general all structures are subjected to different types of loads, usually independent one from the other (permanent loads, variable vertical loads, wind actions, etc.); however in the following chapters for convenient simplification the loads intensity will be described by only one parameter λ called load multiplier. This does not mean that all external forces have to be increased by the factor λ, but in the following cases specific load patterns will be defined, differentiating the group of permanent loads that will be kept constant and a group of variable loads increased proportionally to the load multiplier λ. Such patterns depend on the scope of the analysis, for example if a designer wants to evaluate the safety margin of a structure with respect to seismic actions, a convenient pattern will be to keep constant all the vertical loads (permanent and variable combined by means of suitable coefficients) and to increase proportionally to λ the only horizontal forces until collapse.

3.1.5 CONCENTRATED PLASTICITY - THE PLASTIC HINGE

The assumption of a bilinear moment-curvature diagram like the Prandtl diagram implies the idea of plastic hinge. As soon as one cross-section reaches the value M_p, its rotational stiffness drops to zero, the curvature tends to infinite and the internal bending moment cannot increase further. This cross-sectional state can be represented in the structural model as a plastic hinge, a node with free rotation and the plastic bending moment M_p applied.

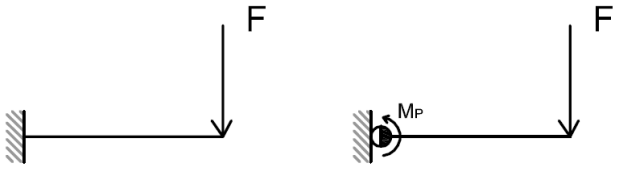

Figure 13 - plastic hinge

3.2 INCREMENTAL PLASTIC ANALYSIS

The first method for an non-linear plastic structural analysis is described in the following paragraphs. As mentioned in the introduction of this chapter the analytical methods will rest on the following hypothesis: small displacement theory, slender elements, shear stresses effect are is neglected, a bilateral moment-curvature diagram M-χ is thus applied, i.e. the flexural behaviour of plastic zones is summarized in plastic hinges.

3.2.1 INCREMENTAL ANALYSIS METHOD

The collapse mechanism can be identified by means of the most intuitive method of plastic analysis, the incremental method: different steps of increasing loads multiplied by the load multiplier λ are applied to the structure. At each phase the loads increments λ_i bring to the formation of a new plastic hinge in the most stressed point of the structure; the computations are performed until the presence of all the plastic hinges make the structure hypostatic.

The critical multiplier λ_{cr} that takes to collapse is given by the sum of load increments λ_i , it is thus determined by the a series of computations performed on linear-elastic structures. The complexity of this method is given by the number of different structural analysis that have to be performed on structures that are different at each step. Some practical examples useful for a better explanation are reported in chapter 4.

3.3 LIMIT PLASTIC ANALYS

The second method to perform a non-linear plastic analysis is based on two theorems presented in the following paragraph. This type of analysis is directly focused on the collapse mechanism, useful to determine the collapse load multiplier λ_{cr}. As previously mentioned both the limit and the incremental plastic analysis method don't take into account rupture criteria and the ultimate rotational capacity of plastic hinges.

3.3.1 THEOREMS OF LIMIT ANALYSIS

KINEMATIC THEOREM – UPPER BOUND

Given an arbitrary collapse mechanism kinematically admissible, if the external work given by the applied loads λ P is equal to the internal one exploited by the plastic hinges, then the factor λ_K, the kinematic multiplier, is equal or greater than the critical load multiplier λ_{cr}.

$$\lambda_{cr} \leq \lambda_K$$

This means that the critical load multiplier λ_{cr} is always lower or equal to any kinematically admissible load multiplier.

STATIC THEOREM – LOWER BOUND

The load multiplier λ_S that gives a bending moment distribution statically admissible is alway lower or at least equal to the critical load multiplier λ_{cr}.

$$\lambda_S \leq \lambda_{cr}$$

This means that the critical load multiplier is always larger than any static admissible one.

CONSEQUENSES OF LIMIT ANALYSIS THEOREMS

The first consequence of the previously mentioned theorems is the uniqueness of the collapse or critical load multiplier. At collapse two circumstances have to be verified: static and kinematical admissibility. The load multiplier that makes true the both previous conditions is unique: let us suppose that two critical loads multiplier are given, $\lambda_1 > \lambda_2$; because of the kinematical theorem $\lambda_1$cannot be larger than λ_2, on the other hand given the static theorem λ_2 cannot be lower than λ_1; it must then be $\lambda_1 = \lambda_2 = \lambda_{cr}$.

The use of the two theorems can take to the definition of a simple method for the resolution of small structures by means of limit analysis that in general ca be sensitively faster than the incremental plastic analysis. A short example is reported in the following lines to better explain the procedure of resolution. It is given a portal frame, with constant cross-section and constant plastic resisting moment M_p.

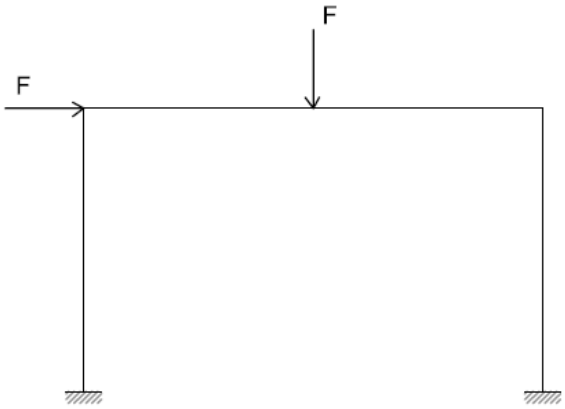

Figure 14 - sample portal frame

- The degree redundancy R is 3;
- The critical cross-sections C where a plastic hinge may appear are 5. The critical cross sections are typically points of application of forces or joints.
- The independent collapse mechanisms are then M=C-R=2.

The collapse mechanisms are the following:

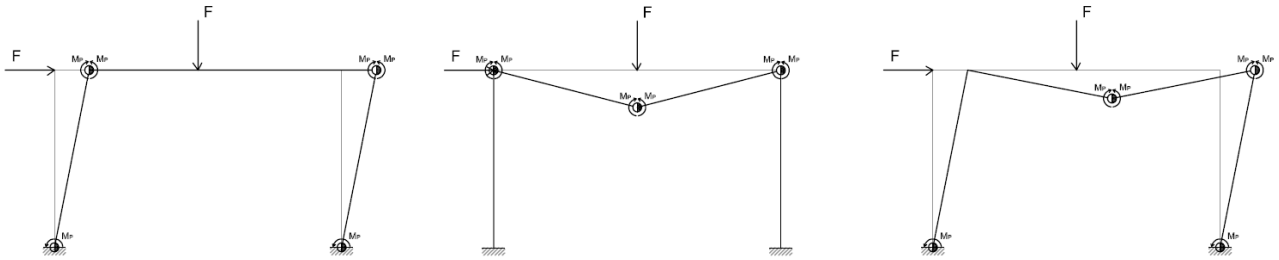

Figure 15 - collapse mechanisms

- The critical load multiplier $\lambda_{cr,i}$ related to the kinematism of each collapse mechanism can be easily computed by the sum of the internal negative virtual works exploited by the plastic hinges and works given by the external forces. For the static theorem the critical load multiplier λ_{cr} will be the lowest.
- In the end a check of the solution can be performed on the bending moment distribution, any value cannot exceed the value M_p.

3.3.2 DISTRIBUTED LOADS

The solution of statically indeterminate structures loaded proportionally by distributed loads presents greater difficulties than structures subjected to concentrated forces. Recalling the procedure described in the previous paragraph, the complexity is the computation of critical cross-sections. There is not any systematic method, the only possibility might be given by a trial and error procedure or the analysis of the bending moment distribution maximums and minimums.

3.3.1 RUPTURE ANALYSIS – NON-INFINITELY DUCTILE STRUCUTRES

Both the incremental method, and the limit analysis described in the following paragraphs, lean on the use of plastic hinges that imply an infinitely ductile material. In fact even the most ductile material has an ultimate strain ε_u that may be reached in the most stressed fibres in the plastic zones, this means that the both analysis methods are completely insensitive to the ultimate strain condition but are based on pure kinematical assumptions. It is to be reported that some methods[1] are available to define the ultimate rotation explicable by a plastic hinge and to compare the value with the one required reaching the ultimate condition. Such procedures undergo the name of rupture analysis methods. This approach may be of interest in determining a unique solution to the "paradox of plastic hinge method" reported in paragraph 2.1.2.

3.3.2 DEPENDENCE OF λ_{CR} ON COERCIVE STATES

Given that the critical load multiplier λ_{CR} is unique and depends on the only value of loads and plastic bending moments, it may be to infer that the coercive states of redundant structures such as thermal effects or constraints displacements do not influence the magnitude of the ultimate load multiplier. This is consequence of the loss of structural redundancy at the formation of each plastic hinge, until the collapse that is related to an hypostatic structure, i.e. not really sensitive to coercive states. Even if the previous statements[2] appear to be consistent, further remarks on this topic are reported in the following chapter.

[1] P. Pozzati C. Ceccoli, *Teoria e tecnica delle strutture vol. 3*, paragraph 3.6
[2] P. Pozzati C. Ceccoli, *Teoria e tecnica delle strutture vol. 3*, paragraph 3.7.2

3.4 RELIABILITY OF STRUCTURES

Many modern construction standards are based on semi-probabilistic approaches, i.e. loads and resistances are no longer taken as deterministic values but rather as random variables with their distributions. In the framework of this thesis it would be of interest to introduce some basic concepts related to the evaluation of the reliability of structural systems. The term "structural system" is referred to structures composed of many members or elements, each one to be verified under different limit states. Moreover there may exist limit states concerning the structure as a whole, which means that the reliability evaluation needs to consider multiple and perhaps correlated limit states.

The failure of a structural system may be define by a number of different criteria such as:

- maximum permissible stress in any point of the structure;
- plastic collapse mechanism formed;
- imposing a limit on the reduction of stiffness;
- maximum deflection;
- damage accumulation reaches a limit state (e.g. fatigue).

Member or cross-sectional failure events defined as before may be combined into failure modes in order to investigate the structural reliability as a whole. When all failure modes are identified, each failure event may be organized in order to form a sort of fault-tree diagram that can highlight logical relations between events. In order to define system reliability or its probability of failure as a function of the probability of failure of its components, two simple concepts may be involved: series and parallel systems. This types of systems are described in the following paragraphs.

3.4.1 SERIES SYSTEMS

In a series system, also called "weakest link" system, the system failure is reached when at least one component reaches its limit state. This concept can be depicted as a chain under traction, where the system resistance is given by the weakest ring resistance. This means that the probability of failure of the system can be combined by means of an OR logical link as follows:

$$P_f = P(F_1 \cup \dots \cup F_i \cup \dots \cup F_N)$$

The probability of failure can be written as a function of the reliability of the system:

$$P_f = 1 - R_{sys}$$

The reliability of the system is attained when all its components are in safe condition, described by the logical ling AND:

$$R_{sys} = (R_1 \cap \dots \cap R_i \cap \dots \cap R_N)$$

If all the reliabilities of the components are statistically independent:

$$R_{sys} = (R_1 \cap \dots \cap R_i \cap \dots \cap R_N) = \prod_{i=1}^{N} R_i = \prod_{i=1}^{N} \left(1 - P_{f,i}\right)$$

Given that for each i[th] component it holds that: $R_i = \left(1 - P_{f,i}\right)$

In the end the probability of failure of a series system of statistically independent elements can be written as a function of the probability of failure of its components as:

$$P_f = 1 - R_{sys} = 1 - \prod_{i=1}^{N} \left(1 - P_{f,i}\right)$$

This expression is the basis for the analysis of the probability of failure distribution of brittle materials [Weibull, 1939]. The series system model is suitable for structures with brittle behaviour, where the failure of a single component leads to a sudden internal redistribution of forces that triggers the so called "progressive failure". It is to be noticed that this formulation may not apply for a system with a large number of brittle elements, where the strength reserve might be large and depending on the single study case.

3.4.2 PARALLEL SYSTEMS

In a parallel system the failure of a single element does not take to the failure of the whole system. This possibility is given by the redundancy of elements. Two types of redundancy can be defined: by "active redundancy" is named a system where all elements participate even in low loading phases; the "passive (or stand-by or fail-safe) redundancy" occurs when the redundant elements participate only to prevent failure of the system.

The failure of a parallel system denoted by active redundancy if given by the logic connector AND, as far as all elements must fail to attain the global failure:

$$P_f = P(F_1 \cap \dots \cap F_i \cap \dots \cap F_N)$$

If the probabilities $P_{f,i}$ of failure of the single elements are statistically independent, the probability of failure of the whole system can be written as a function of the probability of failure of the single elements as:

$$P_f = P(F_1 \cap \dots \cap F_i \cap \dots \cap F_N) = \prod_{i=1}^{N} P_{f,i}$$

It has to be reported that the definition of parallel system is not given by the only geometrical configuration or material characteristics, but is dependent on several factors such as relative stiffness and resistance of members, the local but also the global ductility of a system. It is thus complex to typify a single feature that a system needs to be defined as a parallel system, the key

is rather to understand the relative behaviour of elements and the way they interact inside the system.

3.4.3 DUCTILE BEHAVIOUR & STRUCTURAL SAFETY

The classical approach to structural analysis based on linear-elastic relationships is conducted in order to assure the structure to be not damaged in all its point. This means that the general design approach is to keep the stress level under exercise loads μ_{ex} as a rate γ_{EL} of the elastic limit[3] μ_{EL}.

$$\mu_{ex}{}^{I} = \mu_{EL}/\gamma_{EL}$$

As far as it is function of stress level in the most stressed point of a structure, the reduction factor γ_{EL} can be defined as a local safety factor.

This approach was exposed to strong critiques, given the fact that actions that may have different importance in terms of collapse or damage are not given the proportioned burden.

On the contrary the limit analysis can be employed to define the exercise stress level μ_{ex} as a rate of the collapse load μ_{PL}:

$$\mu_{ex}{}^{II} = \mu_{PL}/\gamma_{PL}$$

In this case the reduction factor γ_{PI} depicts the behaviour of the whole structure, it can be thus defined as a global safety factor. The benefit of this approach is to have a clear view of the structure as a whole, focusing the analysis on failure modes. Some drawbacks are present as well: the simplicity of Prandtl diagram, local failure modes are difficult to be identified given the randomness of accidental loads, the difficulty of identifying failure modes of complex structures.

The two criteria may seem detached and independent, based on different analysis methods, but in fact they are more related than expected. It has to be noticed that the global reduction factor γ_{PI} may present a strong deterioration in time given the unavoidable repetition of stresses increments given by accidental loading. An effective tool to limit the damage given by exercise loading is the local safety factor γ_{EL} because it describes exactly the elastic behaviour until yielding at any point of the structure. On the matter of the dualism of elastic analysis and limit plastic analysis William Prager[4] expressed his point in a congress in Warsaw in 1972: "*This might be the moral of our times: we are experiencing an extremely rapid development of new theories of material mechanics. While one or the other can arise, for engineers, the importance*

[3] As previously reported in the paragraph 3.1.3 the elastic limit is given by the first yielding of any fibre inside the cross-section or in general the first yielding point in a structure.
[4] *Symposium on Foundations of plasticity*, 1972 Warsaw

of linear-elasticity, we have to ponder carefully before abandoning the old, but maybe still incomplete theories that can cover a crucial role".

It is to remark how the limit or plastic approach does not replace completely the linear-elastic one but the both have to contribute to the full understatement of the structural behaviour: not only because the first one is suitable to catch the collapse behaviour and the second one describes carefully the structural response under service loads, but also because the two approaches together can clarify the link between the local behaviour of single elements and the global structural performance under different loading phases.

4. THE ANALYTICAL STUDY

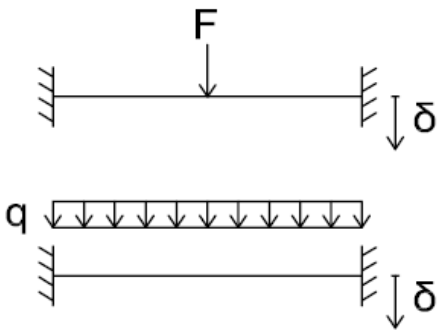

Figure 16 – sample structures

In order to show how the ultimate or collapse load of some simple structures, infinitely ductile, investigated by means if both limit and incremental plastic analysis is not affected by imposed deformations the following study case is investigated. A slender beam, long L, fixed at the ends, subjected in the first example to a concentrated force F (Figure 16 top), in the second to a distributed load q (Figure 16 bottom) which are increased until reaching collapse in presence of an imposed lowering δ on the right side.

4.1 LIMIT PLASTIC ANALYSY

In the first chapter the example of limit plastic analysis is reported in order to understand the expected value of ultimate load multiplier for the two examples. In the limit plastic analysis the presence of the lateral lowering δ is neglected because in the computation of the collapse load multiplier F_U, the virtual works are not sensitive to imposed displacements.

4.1.1 FIRST EXAMPLE – CONCENTRATED LOAD

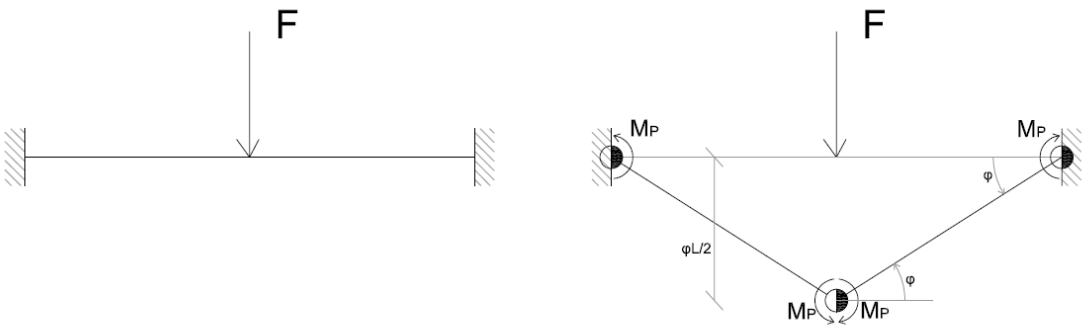

Figure 17 - collappse mechanism

The degree of redundancy R is 2 in the vertical direction, the critical cross-sections C are 3, this means that the independent failure mechanisms are M=C-R=1. The mechanism is depicted in the Figure 17. The collapse load is to be evaluated by means of the virtual works: given the

kinematism, the external virtual work is given by $F_u * \varphi \frac{L}{2}$ and the internal virtual work exploited by the plastic moments is $-4M_P * \varphi$ the ultimate condition is given by the sum of virtual works:

$$F_u * \varphi \frac{L}{2} - 4M_P * \varphi = 0 \;\rightarrow\; F_u = \frac{8M_P}{L}$$

This collapse mechanism is also statically admissible because the bending moment distribution never exceeds the value M_P, the ultimate loading capacity of a beam is thus $F_u = \frac{8M_P}{L}$.

4.1.2 SECOND EXAMPLE – DISTRIBUTED LOAD

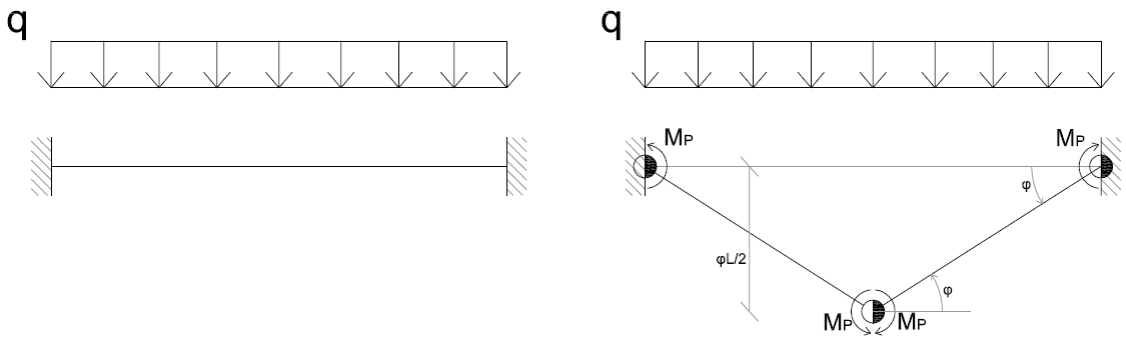

Figure 18 - collapse mechanism

For the second example, the degree of redundancy R is still 2 in the vertical direction, the critical cross-sections C are 3, this means that the independent failure mechanisms are M=C-R=1. The position of the central plastic hinge is a first try, the idea is to put it in the position of maximum expected bending moment; in the following paragraphs it will be demonstrated that its position in exactly in the centre of the beam and is independent on the displacement δ. The mechanism is depicted in the Figure 18. The collapse load is to be evaluated by means of the virtual works: given the kinematism, the external virtual work is given by $q_u * \varphi \frac{L^2}{8}$ and the internal virtual work exploited by the plastic moments is $-4M_P * \varphi$ the ultimate condition is given by the sum of virtual works:

$$q_u * \varphi \frac{L^2}{4} - 4M_P * \varphi = 0 \;\rightarrow\; q_u = \frac{16M_P}{L^2}$$

This collapse mechanism is also statically admissible because the bending moment distribution never exceeds the value M_P, the ultimate loading capacity of a beam is thus $q_u = \frac{16M_P}{L^2}$.

4.2 INCREMENTAL PLASTIC ANALYSIS

4.2.1 FIRST EXAMPLE – CONCENTRATED LOAD

FIRST PHASE

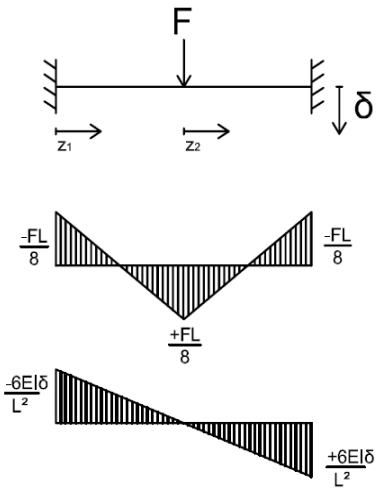

Figure 19 - first phase bending moment distribution

In the first phase, the structure is totally elastic and, in order to represent the magnitude of the lowering δ, the following parameters are defined:

- δ_y is the lowering that would yield the two extremities of the beam, given the bending moment distribution M_δ generated by the imposed displacement, and is:

$$M_\delta(L) = |M_\delta(0)| = \frac{6\delta EJ}{L^2}$$

$$if\ M_\delta(L) = |M_\delta(0)| = M_y \quad \rightarrow \quad \delta_y = \frac{M_y\, L^2}{6EJ}$$

- ξ is the grade of displacement applied to the structure:

$$\xi = \frac{\delta}{\delta_y}; \quad \xi \in [0;1]$$

Given the previous expressions, the bending moment distributiongenerated by the lowering δ (Figure 19 lower diagram) can be defined in the reference system z_1 as follows:

$$M_\delta(z_1) = -\frac{6\delta EJ}{L^2} + \frac{12\delta EJ}{L^2}\left(\frac{z_1}{L}\right) = \frac{\delta}{\delta_y}\left(\frac{6\delta_y EJ}{L^2} + \frac{12\delta_y EJ}{L^2}\left(\frac{z_1}{L}\right)\right)$$

$$M_\delta(z_1) = \xi\left(-M_y + 2M_y\left(\frac{z_1}{L}\right)\right) \qquad z_1 \in [0;L]$$

For seek of simplicity the bending moment distribution generated by the force F (Figure 19 upper diagram) can be defined on two different reference systems z_1 and z_2:

$$M_F(z_1) = -\frac{FL}{8} + \frac{FL}{4}\left(\frac{z_1}{L/2}\right) \qquad z_1 \in [0;L/2]$$

$$M_F(z_2) = \frac{FL}{8} - \frac{FL}{4}\left(\frac{z_2}{L/2}\right) \qquad z_2 \in [0;L/2]$$

Given the linear-elastic behaviour of the structure the superimposition of effects can be applied as follows:

$$M_{tot\,1}(z) = M_\delta(z) + M_F(z)$$

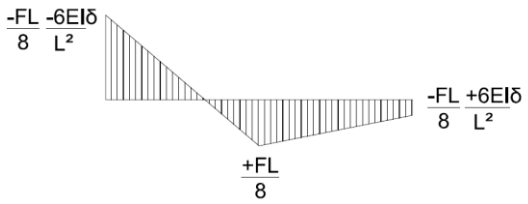

Figure 20 - first phase

As far as the both M_δ and M_F diagrams are represented by liner functions, only three critical cross-section can be immediately identified as possible location of the plastic hinges as they always represent the local minimum or maximum. The three cross sections are z_1=0, z_1=L/2 and z_1=L. The diagram M_{tot} shows the total bending moment distribution in the first phase:

$$M_{tot\,1}(0) = -\frac{FL}{8} - \frac{6\delta EJ}{L^2} = -\frac{FL}{8} - \xi M_y$$

$$M_{tot\,1}(L/2) = +\frac{FL}{8}$$

$$M_{tot\,1}(L) = -\frac{FL}{8} + \frac{6\delta EJ}{L^2} = -\frac{FL}{8} + \xi M_y$$

The first plastic hinge will appear in z=0 because the largest bending moment in magnitude is clearly $M_{tot\,1}(0) = -\frac{FL}{8} - \xi M_y$.

The value of the first load step F_1 is easyly computed as follows:

$$M_{tot\,1}(0) = -\frac{F_1 L}{8} - \xi M_y = M_y$$

$$\rightarrow \quad F_1 = \frac{8M_y}{L}(1-\xi)$$

SECOND PHASE

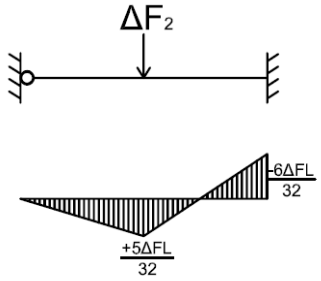

Figure 21- second phase

As far as the first plastic hinge appeared in z=0, for further increments ΔF_2, the structure will behave like the one in Figure 21, with an hinge in z=0, and fixed in z=L. Given the previous discussion about the linear distribution of the bending moment, the only two remaining cross-sections, z=L/2 and z=L, will be investigated. For further increments ΔF_2 :

$$M_{\Delta F_2}(L/2) = +\frac{5\,\Delta F_2 L}{32}$$

$$M_{\Delta F_2}(L) = -\frac{6\,\Delta F_2 L}{32}$$

To the further increments ΔF_2 the bending moment from the first phase is added as follows:

$$M_{tot\,2}(L/2) = M_{tot\,1}(L/2) + M_{\Delta F_2}(L/2) = +\frac{F_1 L}{8} + \frac{5\,\Delta F_2 L}{32}$$
$$M_{tot\,2}(L) = M_{tot\,1}(L) + M_{\Delta F_2}(L) = -\frac{F_1 L}{8} + \xi M_y - \frac{6\,\Delta F_2 L}{32}$$

Given that from the first phase the load multiplier F_1 is: $F_1 = \frac{8M_y}{L}(1-\xi)$

$$M_{tot\,2}(L/2) = +\frac{F_1 L}{8} + \frac{5\,\Delta F_2 L}{32} = M_y(1-\xi) + \frac{5\,\Delta F_2 L}{32}$$
$$M_{tot\,2}(L) = -\frac{FL}{8} + \xi M_y - \frac{6\,\Delta F_2 L}{32} = -M_y + 2\xi M_y - \frac{6\,\Delta F_2 L}{32}$$

The simplest way to find the second load multiplier is to impose that $M_{tot\,2}(z) = M_y$ for both z=L/2 and z=L. The lowest value of ΔF_2 will be the correct one.

$$M_{tot\,2}(L/2) = M_y(1-\xi) + \frac{5\,\Delta F_2 L}{32} = +M_y \quad \rightarrow \quad \Delta F_2 = \frac{32}{5}\,\frac{\xi M_y}{L}$$

$$M_{tot\,2}(L) = -M_y + 2\xi M_y - \frac{6\,\Delta F_2 L}{32} = -M_y \quad \rightarrow \quad \Delta F_2 = \frac{32}{3}\,\frac{\xi M_y}{L}$$

As far as $\frac{32}{5}\,\frac{\xi M_y}{L} < \frac{32}{3}\,\frac{\xi M_y}{L}$, the second plastic hinge appears in z=L/2 and the second load multiplier is:

$$\Delta F_2 = \frac{32}{5}\,\frac{\xi M_y}{L}$$

THIRD PHASE

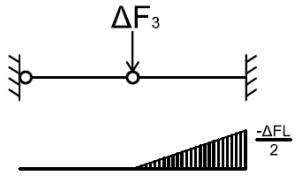

Figure 22 - third phase

For further load increments ΔF_2 the structure reacts as shown in Figure 22, as a cantilever element, subjected to a vertical force on its end, as far as the left portion of the beam does not offer any vertical reaction, given the presence of two subsequent hinges. The bending moment distribution is clearly triangular and reaches its maximum in the fixed end:

$$M_{\Delta F_3}(L) = -\frac{\Delta F_3 L}{2}$$

To the further increments ΔF_3 the bending moment from the first two phases are added as follows:

$$M_{tot\,3}(L) = M_{tot\,2}(L) + M_{\Delta F_3}(L) = -\frac{F_1 L}{8} + \xi M_y - \frac{6\,\Delta F_2 L}{32} - \frac{\Delta F_3 L}{2}$$

Given that from the first two phases the load multipliers F_1 and ΔF_2 are:

$$F_1 = \frac{8M_y}{L}(1-\xi) \quad ; \quad \Delta F_2 = \frac{32}{5}\,\frac{\xi M_y}{L}$$

The bending moment acting on the fixed end in third phase is thus:

$$M_{tot\,3}(L) = M_y(2\xi - 1) - \frac{6}{5}\xi M_y - \frac{\Delta \mathrm{F}_3 L}{2}$$

Imposing the yielding condition $M_{tot}(L)=M_y$, the third load multiplier is computed:

$$M_{tot\,3}(L) = M_y(2\xi - 1) - \frac{6}{5}\xi M_y - \frac{\Delta \mathrm{F}_3 L}{2} = -M_y$$

$$\rightarrow \quad \Delta \mathrm{F}_3 = \frac{8}{5}\ \frac{\xi M_y}{L}$$

The total load multiplier that takes the structure to collapse will be the sum of the three steps previously described:

$$\mathrm{F}_u = \mathrm{F}_1 + \Delta \mathrm{F}_2 + \Delta \mathrm{F}_3 = \frac{8M_y}{L}(1-\xi) + \frac{32}{5}\ \frac{\xi M_y}{L} + \frac{8}{5}\ \frac{\xi M_y}{L} = \frac{8M_y}{L}(1-\xi+\xi) =$$

$$= \frac{8M_y}{L} \qquad \forall\, \xi\ \in [0;1]$$

The value of the ultimate or collapse load F_u is $8\frac{M_y}{L}$ and does not depend on the displacement degree ξ.

4.2.2 SECOND EXAMPLE – DISTRIBUTED LOAD

In the second example the same structure is investigated, subjected to the same lowering δ and to a distributed load q. As previously described (paragraph 3.3.2), in presence of a distributed load the development of the plastic analysis is more complicated, given that the location of local maximum or minimum bending moment may depend on the load q and the lowering δ.

FIRST PHASE

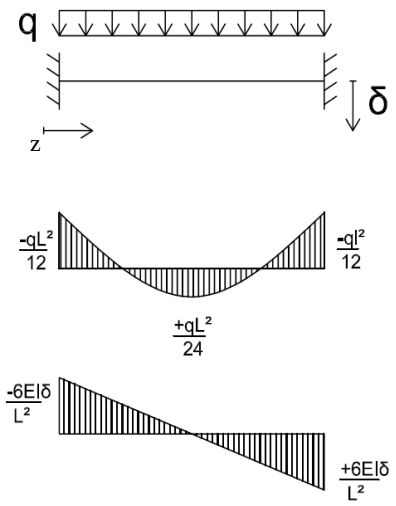

Figure 23 - first phase

In the first phase the structure is totally elastic and, in order to represent the magnitude of the lowering δ, the following parameters are defined:

- δ_y is the lowering that would yield the two extremities of the beam, given the bending moment distribution M_δ generated by the imposed displacement;

$$M_\delta(L) = |M_\delta(0)| = \frac{6\delta EJ}{L^2} \qquad \rightarrow \qquad \delta_y = \frac{M_y\, L^2}{6EJ}$$

- ξ represents the grade of displacement d applied to the structure

$$\xi = \frac{\delta}{\delta_y};\ \xi \in [0;1]$$

Given the previous expressions the bending moment diagrams are defined as follows:

$$M_q(z) = q_1\left(-\frac{z^2}{2} + \frac{zL}{2} - \frac{L^2}{12}\right)$$

$$M_\delta(z) = -\frac{6\delta EJ}{L^2} + \frac{12\delta EJ}{L^2}\left(\frac{z}{L}\right) = -\xi M_y + 2\xi M_y \frac{z}{L}$$

Where M_q is the bending moment generated by the applied distributed load and M_δ generated by the imposed displacement, z is the abscissa starting from the left end, as shown inFigure 23. Given the linear-elasticity of the structure the superimposition of effects can be applied as follows:

$$M_{tot\,1}(z) = M_\delta(z) + M_q(z)$$

$$M_{tot\,1}(z) = q_1\left(-\frac{z^2}{2} + \frac{zL}{2} - \frac{L^2}{12}\right) - \xi M_y + 2\xi M_y \frac{z}{L}$$

In order to define the first load step, the yielding condition will be applied to all the critical cross-sections and the first multiplier will be obtained taking the lowest value from all the critical cross-sections:

$$M_{tot\,1}(z=0) = -\frac{q_1 L^2}{12} - \xi M_y \qquad if\ M_{tot\,1}(0) = -M_y \quad \rightarrow \quad q_1 = 12\frac{M_y}{L^2}(1-\xi)$$

$$M_{tot\,1}(z=L) = -\frac{q_1 L^2}{12} + \xi M_y \qquad if\ M_{tot\,1}(L) = -M_y \quad \rightarrow \quad q_1 = 12\frac{M_y}{L^2}(1+\xi)$$

In order to find the maximum positive bending moment and its location, the first derivative of the bending moment distribution is imposed to be zero:

$$M_{tot\,1}{}'(z) = \frac{2\xi M_y}{L} - q_1 z + \frac{q_1 L}{2} = 0 \quad \rightarrow \quad z_{max} = \frac{L}{2} + \frac{2\xi M_y}{q_1 L}$$

Where z_{max} is the abscissa of the maximum positive bending moment $M_{tot\,1}(z_{max})$:

$$M_{tot\,1}(z_{max}) = \frac{q_1 L^2}{24} + \frac{2\left(\xi M_y\right)^2}{q_1 L}$$

In order to define the firs multiplier the yielding condition is applied to the cross-section in z_{max}:

$$if\ M_{tot\,1}(z_{max}) = \frac{q_1 L^2}{24} + \frac{2\left(\xi M_y\right)^2}{q_1 L} = +M_y \ \rightarrow q_1 = 12\frac{M_y}{L^2}\left(1 \mp \sqrt{1-\frac{\xi^2}{3}}\right)$$

$$if \quad q_1 = 12\frac{M_y}{L^2}\left(1 - \sqrt{1-\frac{\xi^2}{3}}\right) \quad \rightarrow \quad z_{max} > L$$

$$\rightarrow \quad q_1 = 12\frac{M_y}{L^2}\left(1 + \sqrt{1-\frac{\xi^2}{3}}\right)$$

As far as:

$$\left(1 + \sqrt{1-\frac{\xi^2}{3}}\right) > (1-\xi) \qquad \text{and} \qquad (1+\xi) > (1-\xi)$$

The first plastic hinge appears in z=0 and the first load multiplier is:

$$q_1 = 12\frac{M_y}{L^2}(1-\xi)$$

SECOND PHASE Δq_2

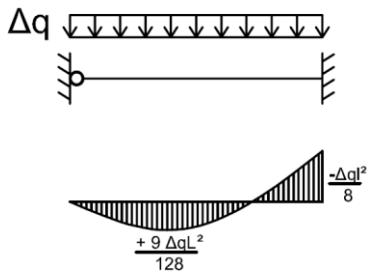

Figure 24 - second phase

For further increments Δq_2 the structure will react as the one represented in Figure 24, with a hinge in z=0. The bending moment distribution will be:

$$\Delta M_{q2}(z) = \Delta q_2 \left(-\frac{z^2}{2} + \frac{3zL}{8}\right)$$

With the maximum and minimum:

$$\Delta M_{q2}(L) = -\frac{\Delta q_2 \, L^2}{8} \quad ; \quad \Delta M_{q2}\left(\frac{3L}{8}\right) = +\frac{9 \, \Delta q_2 \, L^2}{128}$$

To the further increments Δq_2 the bending moment from the first phase is added as follows:

$$M_{tot\,2}(z) = M_{tot\,1}(z) + \Delta M_{q2}(z)$$

$$= q_1 \left(-\frac{z^2}{2} + \frac{zL}{2} - \frac{L^2}{12}\right) - \xi M_y + 2\xi M_y \frac{z}{L} \Delta q_2 \left(-\frac{z^2}{2} + \frac{3zL}{8}\right)$$

Imposing that the first load multiplier is $q_1 = 12\frac{M_y}{L^2}(1-\xi)$:

$$M_{tot\,2}(z) = 12\frac{M_y}{L^2}(1-\xi)\left(-\frac{z^2}{2} + \frac{zL}{2} - \frac{L^2}{12}\right) - \xi M_y + 2\xi M_y \frac{z}{L} \Delta q_2 \left(-\frac{z^2}{2} + \frac{3zL}{8}\right)$$

$$M_{tot\,2}(z) = z^2\left(-\frac{\Delta q_2}{2} - 6\frac{M_y}{L^2}(1-\xi)\right) + z\left(\frac{3\,\Delta q_2 L}{8} + \frac{M_y}{L}(6-4\xi)\right) - M_y$$

As it has been done for the first load step the yielding conditions will be imposed to all the critical cross-sections, the second load multiplier will be the one related to the lower increment Δq_2

$$M_{tot\,2}(L) = -\frac{\Delta q_2 \, L^2}{8} - M_y(1-2\xi) \qquad if\ M_{tot\,2}(L) = -M_y \quad \rightarrow \quad \Delta q_2 = 16\frac{M_y}{L^2}\xi$$

Looking for the maximum positive and its location, the first derivative of the bending moment distribution is imposed to be zero:

$$M_{tot\,2}{}'(z_{max}) = 2z\left(-\frac{\Delta q_2}{2} - 6\frac{M_y}{L^2}(1-\xi)\right) + \left(\frac{3\,\Delta q_2 L}{8} + \frac{M_y}{L}(6-4\xi)\right) = 0$$

$$\rightarrow \quad z_{max} = \frac{L}{2}\left(\frac{\frac{3\,\Delta q_2}{8} + \frac{M_y}{L^2}(6-4\xi)}{-\frac{\Delta q_2}{2} - 6\frac{M_y}{L^2}(1-\xi)}\right)$$

As far as the last expression is complicated to be investigated, it will be imposed that in z=L:

$$M_{tot\,2}(L) = -M_y \qquad \rightarrow \qquad \Delta q_2 = 16\frac{M_y}{L^2}\xi$$

And it will be checked that the positive bending moment is always lower than M_y:

$$M_{tot\,2,max}(z) = M_{tot\,2}(z_{max}) \leq +M_y \quad \forall\, \xi \in [0;1] \quad ; \quad z_{max} = z_{max}\left(\Delta q_2 = 16\frac{M_y}{L^2}\xi\right)$$

It can be shown that, imposing the condition $M_{tot\,2}(L) = -M_y$ the maximum bending moment location z_{max} is always equal to L/2:

$$z_{max}\left(\Delta q_2 = 16\frac{M_y}{L^2}\xi\right) = \frac{L}{2}\left(\begin{matrix}\dfrac{3\cdot 16\frac{M_y}{L^2}\xi}{8} + \dfrac{M_y}{L^2}(6-4\xi) \\ -\dfrac{16\frac{M_y}{L^2}\xi}{2} - 6\dfrac{M_y}{L^2}(1-\xi)\end{matrix}\right) = \frac{L}{2}\left(\begin{matrix}\dfrac{M_y}{L^2}(6+2\xi) \\ \dfrac{M_y}{L^2}(6+2\xi)\end{matrix}\right) = \frac{L}{2}$$

Which leads to:

$$M_{tot\,2,max}(z) = M_{tot\,2}(z_{max}) = +M_y\frac{(1+\xi)}{2} \leq +M_y \quad \forall\, \xi \in [0;1]$$

The second plastic hinge appears in z=L and the second load multiplier is:

$$\Delta q_2 = 16\frac{M_y}{L^2}\xi$$

THIRD PHASE Δq_3

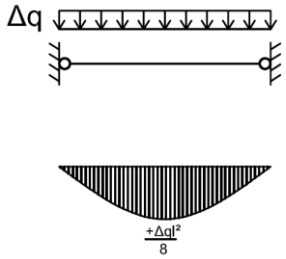

Figure 25 - third phase

For further increments Δq_3 the structure will behave as a simple supported beam, with the following bending moment distribution:

$$\Delta M_{q3}(z) = \Delta q_3\left(-\frac{z^2}{2} + \frac{zL}{2}\right)$$

$$\Delta M_{q3}\left(\frac{L}{2}\right) = \frac{\Delta q_3\, L^2}{8} \quad ; \quad \Delta M_{q3}(0) = \Delta M_{q3}(L) = 0$$

Adding the bending moment from the first two phases:

$$M_{tot\,3}(z) = q_1\left(-\frac{z^2}{2} + \frac{zL}{2} - \frac{L^2}{12}\right) - \xi M_y + 2\xi M_y\frac{z}{L} \Delta q_2\left(-\frac{z^2}{2} + \frac{3zL}{8}\right) + \Delta q_3\left(-\frac{z^2}{2} + \frac{zL}{2}\right)$$

Imposing that the first two load multiplier are $q_1 = 12\frac{M_y}{L^2}(1-\xi)$; $\Delta q_2 = 16\frac{M_y}{L^2}\xi$

The bending moment distribution in the third phase is:

$$M_{tot\,3}(z) = z^2\left[-\frac{M_y}{L^2}(6+2\xi) - \frac{\Delta q_3}{2}\right] + z\left[\frac{M_y}{L^2}(6+2\xi) + \frac{\Delta q_3}{2}\right] - M_y$$

$$M_{tot\,3}(0) = M_{tot\,3}(L) = -M_y$$

As far as the only critical cross-section is the one subjected to the maximum positive bending moment the first derivative of the bending moment is imposed to be equal to zero:

$$M_{tot\,3}{}'(z) = z\left[-\frac{M_y}{L^2}(6+2\xi) - \frac{\Delta q_3}{2}\right] + \left[\frac{M_y}{L^2}(6+2\xi) + \frac{\Delta q_3}{2}\right] = 0$$

And the location of the maximum bending moment z_{max} is computed:

$$\rightarrow \quad z_{max} = \frac{L}{2}\left(\frac{\frac{M_y}{L^2}(6+2\xi) + \frac{\Delta q_3}{2}}{\frac{M_y}{L^2}(6+2\xi) + \frac{\Delta q_3}{2}}\right) = \frac{\left(\frac{M_y}{L^2}(6+2\xi) + \frac{\Delta q_3}{2}\right)}{\left(\frac{M_y}{L^2}(6+2\xi) + \frac{\Delta q_3}{2}\right)} \cdot \frac{L}{2} = \frac{L}{2} \qquad \forall\, \xi \in [0;1]$$

Where the yielding condition is:

$$M_{tot\,3}(z_{max}) = M_{tot\,3}\left(\frac{L}{2}\right) = \frac{\Delta q_3\, L^2}{8} + \frac{M_y}{2}(3+\xi) = M_y$$

That leads to the values

$$\rightarrow \qquad \Delta q_3 = 4\frac{M_y}{L^2}(1-\xi)$$

The third plastic hinge appears in z=L/2 and the third load multiplier is:

$$\Delta q_3 = 4\frac{M_y}{L^2}(1-\xi)$$

The total load multiplier that takes the structure to collapse will be the sum of the three steps previously described:

$$q_u = q_{1+}\Delta q_2 + \Delta q_3 = 12\frac{M_y}{L^2}(1-\xi) + 16\frac{M_y}{L^2}\xi + 4\frac{M_y}{L^2}(1-\xi) = 16\frac{M_y}{L^2} \qquad \forall\, \xi \in [0;1]$$

The value of the ultimate load q_u is $16\frac{M_y}{L^2}$ and does not depend on the displacement degree ξ.

4.3 SOFTWARE IMPLEMENTATION

In order to investigate how the f.e.m. (Sap2000 v.15) results are approximate w.r.t. the previous theoretical development, a practical example is solved for both the previous two examples. Five different lowering degrees will be applied (ξ= 0 ; 0,1 ; 0,5 ; 0,75 ; 1,0) and the results from the software will be compared with the expected theoretical ones.

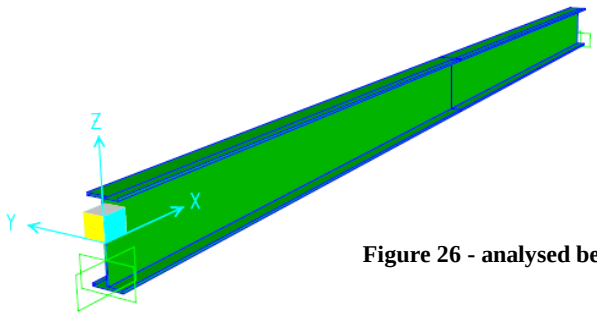

Figure 26 - analysed beam

4.3.1 STRUCTURAL DESCRIPTION

The structure is composed by a single steel beam fixed at the ends, with a span of L=5 m. The mechanical and geometrical parameters are reported in the following table:

Geometry			**Material**		
L	5	m	E	2,00E+08	kN/m^2
h	305	mm		199,9	GPa
b	127	mm	f_y	350	MPa
A	0,0043	m^2	f_u	450	MPa
I_3	6,57E-05	m^4	**Plastic analysis**		
W_e	4,31E-04	m^3	$M_p=W_p*f_y$	171,92	kNm
W_p	4,91E-04	m^3	$M_y=W_e*f_y$	150,96	kNm
W_p/W_e	1,14	-	$\delta_y=\frac{M_p L^2}{6EJ}$	54,53	mm

The cross section is a symmetric double-T with the following dimensions:

- h is the external height;
- b is the flange width;
- A is the cross-sectional area;
- I_3 is the strong-axis moment of inertia;
- W_e and W_p are the elastic and plastic section modules.

The material characteristics correspond to a non-standardized steel (defined for the only theoretical development):

- E is the Young modulus;
- fy and fu are the yielding and maximum stresses.

Given these parameters, the plastic analysis ones are computed as follows:

- $M_p = w_p f_y = 172\ kNm$ is the plastic bending moment;
- $M_y = w_e f_y = 151\ kNm$ is the plastic yielding moment;
- $\delta_y = \frac{M_p L^2}{6EJ}$ is the lowering of the right end that causes the complete yielding of the two fixed ends.

In the development of the theoretical results no distinction was made between M_y and M_p , as far as both the limit and incremental plastic analysis are based on the hypothesis of the Prandtl bending moment – curvature diagram (Figure 27). At the same way, the software applies the same elastic-perfectly plastic behaviour, with the only notation of M_p instead of M_y.

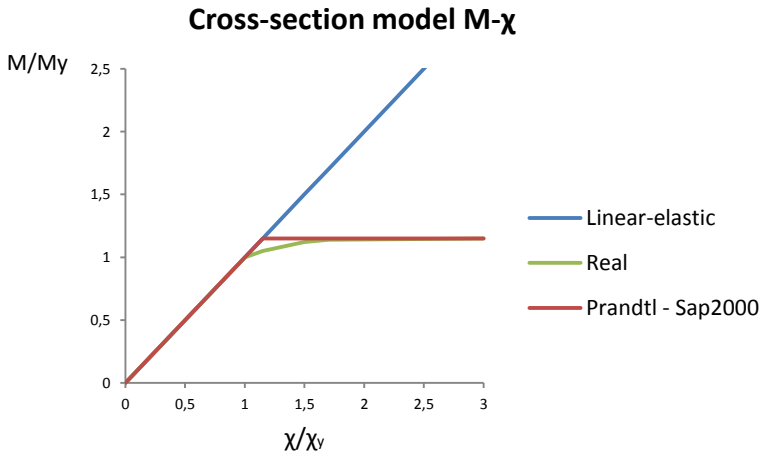

Figure 27 - M-x diagrams

4.3.2 FIRST EXAMPLE – CONCENTRATED FORCE

The theoretical development of first example is described in the previous chapter, the only results are reported here:

$$F_1 = \frac{8M_p}{L}(1-\xi) \quad ; \quad \Delta F_2 = \frac{32}{5}\frac{\xi M_p}{L} \quad ; \quad \Delta F_3 = \frac{8}{5}\frac{\xi M_p}{L}$$

With an ultimate load of:

$$F_u = F_1 + \Delta F_2 + \Delta F_3 = \frac{8M_p}{L} \qquad \forall\, \xi \in [0;1]$$

Given the example structure previously described, the values of the load increments expected for the different lowering grades ξ_i are:

		Theoretical load multiplier [kN]		
$\xi = \delta / \delta_y$	δ [mm]	F1	ΔF2	ΔF3
0	0,00	275,1	0,0	0,0
0,1	5,45	247,6	22,0	5,5
0,5	27,26	137,5	110,0	27,5
0,75	40,89	68,8	165,0	41,3
1	54,52	0,0	220,1	55,0

And the ultimate load $F_u = F_1 + \Delta F_2 + \Delta F_3 = \frac{8M_p}{L} = 275{,}1\ kN \qquad \forall\, \xi \in [0;1]$

SOFTWARE RESULTS

In the following table all the results of a non-linear static analysis are reported, different load cases have been defined in order to subject the structure to the lowering grades $\xi_i = \delta_i / \delta_y$:

$\xi = \delta / \delta_y$	δ [mm]
0	0,00
0,1	5,45
0,5	27,26
0,75	40,89
1	54,52

All the load increments and the central node deflection for each lading stage and lowering grade are reported in the following table and graph:

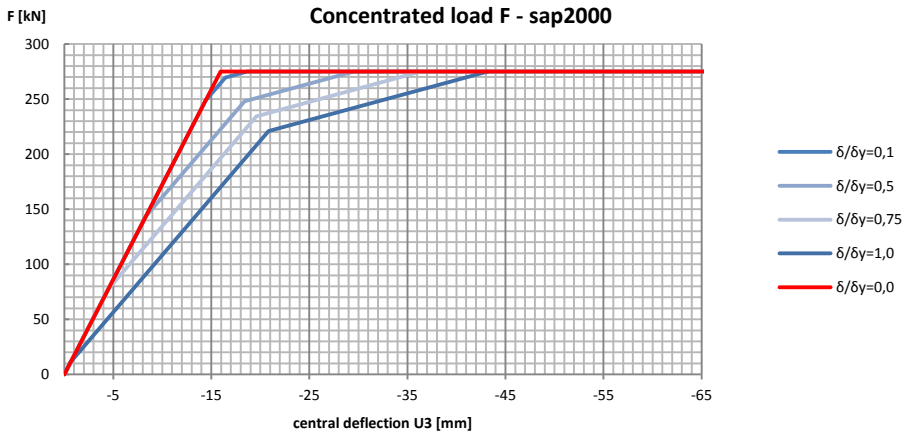

Figure 28 - force displacement graph

δ/δy=0,0			
U3 [m]	ΔU3 [mm]	F [kN]	ΔF [kN]
0	0	0	-
-0,015937	-15,937	275,065	275,065
-0,04927	-49,27	275,065	0
-0,082604	-82,604	275,065	0

δ/δy=0,1			
U3 [m]	ΔU3 [mm]	F [kN]	ΔF [kN]
-0,002725	0	7,105E-15	-
-0,017133	-14,408	248,681	248,681
-0,019153	-16,428	269,656	20,975
-0,021387	-18,662	275,065	5,409
-0,10472	-101,995	275,065	0

δ/δy=0,5			
U3 [m]	ΔU3 [mm]	F [kN]	ΔF [kN]
-0,01363	0	-1,421E-14	-
-0,021921	-8,291	143,095	143,095
-0,03202	-18,39	248,011	104,916
-0,043197	-29,567	275,065	27,054
-0,12653	-112,9	275,065	0

δ/δy=0,75			
U3 [m]	ΔU3 [mm]	F [kN]	ΔF [kN]
-0,020445	0	7,105E-15	-
-0,024913	-4,468	77,111	77,111
-0,040062	-19,617	234,484	157,373
-0,056827	-36,382	275,065	40,581
-0,14016	-119,715	275,066	0,001

δ/δy=1,0			
U3 [m]	ΔU3 [mm]	F [kN]	ΔF [kN]
-0,02726	0	1,421E-14	-
-0,027905	-0,645	11,126	11,126
-0,048104	-20,844	220,957	209,831
-0,070457	-43,197	275,065	54,108
-0,070457	-43,197	275,065	54,108

As it is evident, all the ultimate loads F_u computed by the software are equal and do not depend on the lowering grade ξ , as expected. In order to evaluate the real efficiency of the non-linear analysis of the software, in the following table are reported and compared all the load increments ΔF:

	Theoretical [kN]			Sap2000 [kN]				error		
ξ =δ/δy	F_1	ΔF_2	ΔF_3	F_1	ΔF_2	ΔF_3	Fu	F_1	ΔF_2	ΔF_3
0	275,1	0,0	0,0	275,1	0,0	0,0	275,1	0%	0%	0%
0,1	247,6	22,0	5,5	248,7	21,0	5,4	275,1	0%	0%	0%
0,5	137,5	110,0	27,5	143,1	104,9	27,1	275,1	-2%	2%	0%
0,75	68,8	165,0	41,3	77,1	157,4	40,6	275,1	-3%	3%	0%
1	0,0	220,1	55,0	11,1	209,8	54,1	275,1	-4%	4%	0%
	Fu	275,1	kN							

4.3.3 SECOND EXAMPLE – DISTRIBUTED LOAD

The theoretical development of first example is described in the previous chapter, the only results are reported here:

$$q_1 = 12\frac{M_p}{L^2}(1-\xi) \quad ; \quad \Delta q_2 = 16\frac{M_p}{L^2}\xi \quad ; \quad \Delta q_3 = 4\frac{M_p}{L^2}(1-\xi)$$

With an ultimate load of:

$$q_u = q_{1+}\Delta q_2 + \Delta q_3 = 16\frac{M_p}{L^2} \qquad \forall\, \xi \in [0;1]$$

Given the example structure previously described, the values of the load increments expected for the different lowering grades ξ_i are:

		Theoretical load multiplier [kN/m]		
δ/δy	d [mm]	qL1	ΔqL2	ΔqL3
0,0	0,0	82,5	0,0	27,5
0,1	5,5	74,3	11,0	24,8
0,5	27,3	41,3	55,0	13,8
0,8	40,9	20,6	82,5	6,9
1,0	54,5	0,0	110,0	0,0
		qu	110,0	kN/m

And the ultimate load $q_u = q_{1+}\Delta q_2 + \Delta q_3 = 16\frac{M_p}{L^2} = 110{,}0\ {}^{kN}/_{m} \qquad \forall\, \xi \in [0;1]$

SOFTWARE RESULTS

In the following table all the results of a non-linear static analysis are reported, different load cases have been defined in order to subject the structure to the lowering grades $\xi_i=\delta_i/\delta_y$:

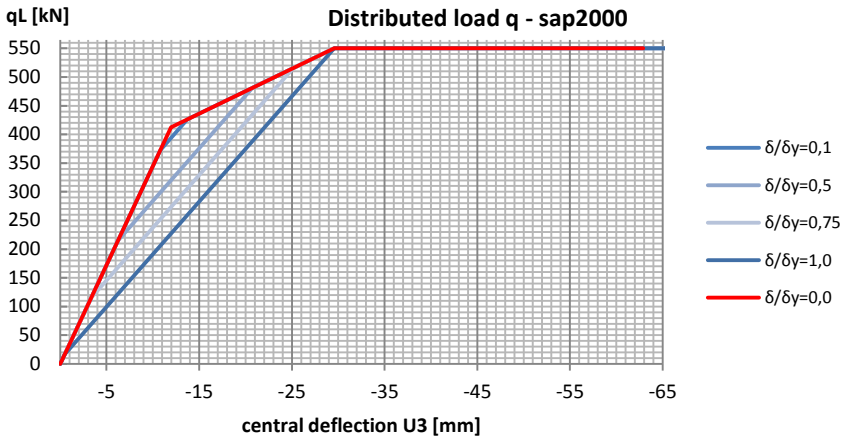

Figure 29 - force-displacement graph

δ/δy=0,0			
U3 [m]	ΔU3 [mm]	qL [kN]	Δq [kN]
0	0	0	-
-0,011953	-11,953	412,597	82,52
-0,029564	-29,564	550,13	27,51
-0,062897	-62,897	550,13	0,00

δ/δy=0,1			
U3 [m]	ΔU3 [mm]	qL [kN]	Δq [kN]
-0,002725	0	7,105E-15	-
-0,013531	-10,806	373,021	74,60
-0,016439	-13,714	426,349	10,67
-0,032289	-29,564	550,13	24,76
-0,115622	-112,897	550,131	0,00

δ/δy=0,5			
U3 [m]	ΔU3 [mm]	qL [kN]	Δq [kN]
-0,01363	0	-1,421E-14	-
-0,019848	-6,218	214,643	42,93
-0,03439	-20,76	481,379	53,35
-0,043194	-29,564	550,13	13,75
-0,126527	-112,897	550,131	0,00

δ/δy=0,75			
U3 [m]	ΔU3 [mm]	qL [kN]	Δq [kN]
-0,020445	0	7,105E-15	-
-0,023796	-3,351	115,666	23,13
-0,045609	-25,164	515,769	80,02
-0,050009	-29,564	550,13	6,87
-0,133342	-112,897	550,131	0,00

δ/δy=1,0			
U3 [m]	ΔU3 [mm]	qL [kN]	Δq [kN]
-0,02726	0	1,421E-14	-
-0,027743	-0,483	16,689	3,34
-0,056825	-29,565	550,101	106,68
-0,140158	-112,898	550,102	0,00
-0,193095	-165,835	550,102	0,00

As it is evident, all the ultimate loads q_u computed by the software are equal and do not depend on the lowering grade ξ , as expected.

The value is correct, $q_u\, L = 16\frac{M_p}{L^2}L = 110{,}0 \cdot 5\ kN = 550{,}0 \qquad \forall\, \xi\ \in [0;1]$

In order to evaluate the real efficiency of the non-linear analysis of the software, in the following table are reported and compared all the load increments ΔF:

	Theoretical [kN/m]			Sap2000 [kN/m]				Error		
δ/δy	qL1	ΔqL2	ΔqL3	qL1	ΔqL2	ΔqL3	qu	qL1	ΔqL2	ΔqL3
0,0	82,5	0,0	27,5	82,5	0,0	27,5	110,0	0%	0%	0%
0,1	74,3	11,0	24,8	74,6	10,7	24,8	110,0	0%	0%	0%
0,5	41,3	55,0	13,8	42,9	53,3	13,8	110,0	-2%	2%	0%
0,8	20,6	82,5	6,9	23,1	80,0	6,9	110,0	-2%	2%	0%
1,0	0,0	110,0	0,0	3,3	106,7	0,0	110,0	-3%	3%	0%
	qu	110,0	kN/m							

4.4 BRITTLE BEHAVIOUR & CONCLUSIONS

All the previous examples and computations have been performed under the assumption of infinite ductility. On the other hand if the components are thought to be brittle, i.e. failure happens as soon as the maximum capacity is reached, the maximum bearing capacity decreases linearly with the initial displacement grade ξ. In particular the first load increment in order to reach the formation of the first plastic hinge, if applied to a brittle beam, it represents the collapse load.

For the concentrated load, the bearing capacity of a brittle beam is given by:

$$F_1 = F_U = \frac{8M_P}{L}(1-\xi)$$

While in the case of a ductile beam the ultimate load bearing capacity is:

$$\mathrm{F}_u = \mathrm{F}_1 + \Delta\mathrm{F}_2 + \Delta\mathrm{F}_3 = \frac{8M_P}{L} \qquad \forall\, \xi \in [0;1]$$

For the distributed load, the bearing capacity of a brittle beam is given by:

$$q_1 = q_U = 12\frac{M_y}{L^2}(1-\xi)$$

While in the case of a ductile beam the ultimate load bearing capacity is:

$$q_u = q_{1+}\Delta q_2 + \Delta q_3 = 16\frac{M_y}{L^2} \qquad \forall\, \xi \in [0;1]$$

In this first simple example the ductility has the double benefit of increasing the perfect structure (i.e. in case of $\xi = 0$) bearing capacity in case of distributed load from $12\frac{M_y}{L^2}$ to $16\frac{M_y}{L^2}$ and in second place to make the ultimate load of ductile structures insensible on the initial displacement grade ξ.

5. CONCRETE FRAME

The previous case can be generalized to a more complex structure: in the following chapter a reinforced concrete frame will be subjected to an initial settlement configuration and then to a vertical push-over analysis in order to determine its vertical ultimate resistance. Different ductility levels will be given to the elements composing the frame in order to understand the relation between ductility and ultimate bearing capacity in presence of increasing settlement of supports. The aim of this analysis is not strictly related to the design of the frame components but, given some cross-section geometries and their resistance parameters, to report the ultimate bearing capacity, i.e. the maximum load multiplier λ_Q, as a function of both settlement ratio ξ and elements ductility μ_{el}.

$$\lambda_Q = \lambda_Q(\xi\ ;\ \mu_{el})$$

5.1 STRUCTURE DESCRIPTION

5.1.1 GEOMETRICL DESCRIPTION

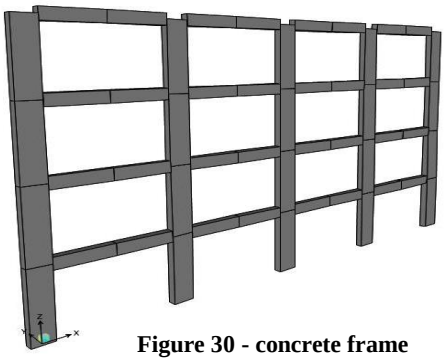

Figure 30 - concrete frame

The frame is composed of four storeys and four spans, the spans are equally distributed and have a length of 5 meters, the inter-storey distance is 3,1 meters. The frame has been thought as principal resisting part of a building having transversal slabs 6 meters long, the vertical loads will be thus given to the frame as linear loads, coming from a distributed load multiplied by a influence length of 6 meters.

5.1.2 MATERIAL PROPERTIES

The materials composing the structures are the most common ones used in the design of ordinary buildings: the concrete is of class C25/30 while the reinforcement steel is of class B 450 C. the me4chanical parameters are reported in the following tables:

CONCRETE	C30/37		STEEL	B450C	
fck	25	N/mm2	**fyk**	450	N/mm2
fcd	14,2	N/mm2	**fyd**	391,30	N/mm2
fctm	2,6	N/mm2	**Agt**	7,50	%
fctk	1,8	N/mm2	**εud**	6,75	%
εcu	0,35	%	**εyd**	0,196	%
Ecm	31	Gpa	**Es**	200	Gpa

5.1.3 CROSS-SECION PROPERTIES

In order to define two different cases two different types of frame will be defined and subjected to the same loading configurations: one case where beams are weaker than columns and a second one where beams are stronger than columns. To obtain such a behaviour the cross-sections of elements will differ in the two cases.

As expressed in the paragraph 3.2 the collapse load is obtained focusing on the only flexural resistance of elements, i.e. the shear resistance is thought to be sufficiently higher than the flexural one in order to obtain a only flexural failure.

WEAK BEAM CASE

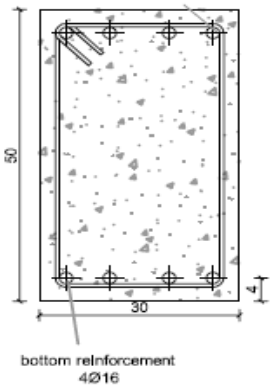

In the first case the beam is in averagely[5] weaker than the column. Its cross section is 30 cm wide and 50 cm high, the top reinforcement is placed at 4 cm from the top fibre, the bottom one at a distance d of 46 cm. Both the top and the bottom reinforcement are composed of 4 bars of a diameter of 16 mm (4Φ16), corresponding to an area of $A_s = A_s = 8{,}04\ cm^2$. The resisting bending moment M_{Rd}=135,9 kNm.

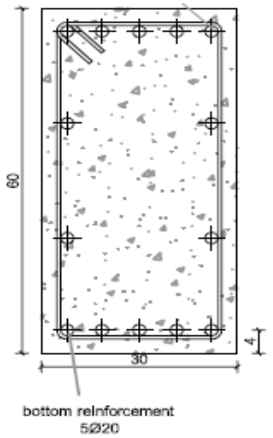

In order to be more resistant than the beam, the column has a cross-sectional width of 30 cm and a depth of 60 cm, the reinforcement is placed in four layers, the external ones 4 cm far from the concrete edge hold 5 bars with a diameter of 20 mm (5Φ20), the internal layers have only two Φ20 bars. The external layers are the ones that provide the major part of the bending resistance have a steel area of $A_s = A_s = 15{,}7\ cm^2$. The M_{Rd}-N_{Rd} diagram for the column is depicted as follows.

Figure 31 - r.c. sections details

[5] The column flexural resistance is function of the normal force applied, in this case the column is stronger than the beam for normal forces in between 0 and 0,85 N_{Rd}

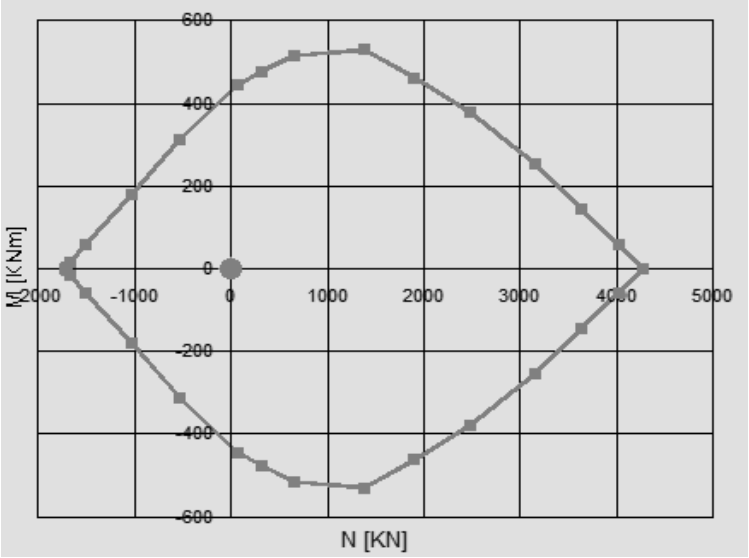

Figure 32 - M-N diagram "weak beam" case

WEAK COLUMN CASE

In order to have a more complete description of the phenomenon also the case of weak column is investigated. In this configuration the crisis appears in the column sections, where the interaction M-N is more relevant and thus the procedure is more complex.

The beam cross-section in this case maintains the same dimensions, while the reinforcement is increased. The both top and bottom reinforcement are composed of 4Φ20 bars, with a total area of reinforcement of $A_s = A_s = 12{,}6\ cm^2$. The resisting bending moment is thus M_{Rd}=209,7 kNm.

In order to decrease the bending resistance trying to avoid the collapse for excessive normal force, the dimensions of the column cross-section have been changed. The height is reduced to 40 cm, while the width is increased to 40 cm. the reinforcement ratio is kept reasonably low, $A_s = A_s = 8{,}04\ cm^2$. The M_{Rd}-N_{Rd} diagram for the column is depicted as follows.

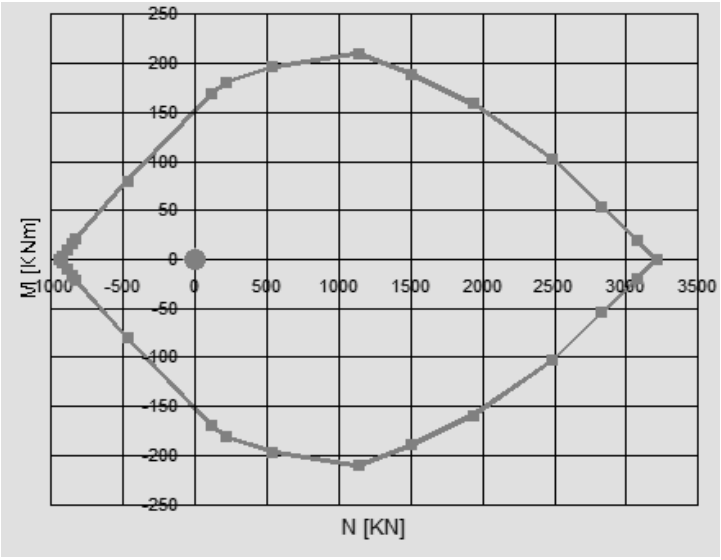

Figure 33 - M-N diagram "weak column" case

5.2 ACTIONS

The actions applied to the structure are taken from an average civil building, with hollow-clay blocks slabs, an ordinary non-structural layering at each floor, and office accidental loads proposed by the Italian standard.

In the framework of the thesis some initial differential settlements are imposed to the structure together with the permanent loads. The accidental load Q is then increased until failure of the structure. The ultimate or critical load multiplier λ_Q will be then reported and compared.

5.2.1 VERTICAL LOADS

As previously mentioned all the vertical loads are usual values for civil buildings. As far as the aim of this analysis is not the design of a particular structure but the investigation on its behaviour in ultimate conditions, the magnitude of loads is not a crucial parameter but it is reported for a complete description of the procedure.

The permanent structural loads are given by the self-weight of beam and columns ($\gamma_{RC} = 25\ {}^{kN}/_{m^3}$) and by the resisting section of slabs, evaluated equal to 3,15 ${}^{kN}/_{m^2}$. The influence length is thought to be 6 meters. The structural load $G_{1,k}$ given by the slab to the frame is thus 18,9 ${}^{kN}/_{m}$.

The permanent non-structural load $G_{2,k}$ is evaluated as 4,2 ${}^{kN}/_{m^2}$ on the slab, the frame is thus subjected to 25,2 ${}^{kN}/_{m}$.

The variable load Q suggested by the Italian standards is 3,0 ${}^{kN}/_{m^2}$ translated into 18 ${}^{kN}/_{m}$ on the frame.

5.2.2 SETTLEMENT CONFIGURATIONS

In order to evaluate the impact of initial coercive states on the structure, two different settlement configurations have been imposed to the concrete frame. The shapes have been normalized on the highest displacement, and then scaled by the parameter $\xi\ \delta_y = \left(\frac{\delta}{\delta_y}\right)\delta_y$ which gives the initial stress level.

SETTLEMENT CONFIGURATION 1

The first differential settlement configuration is a linear anti-symmetric distribution of settlements, increasing on one side. The shape is depicted in Figure 34.

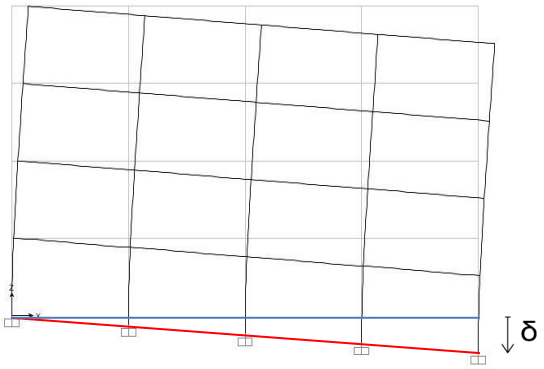

Figure 34 - settlement configuration 1

The five supports from left to right are subjected to a settlement following the pattern δ (0; 0,25; 0,5; 0,75; 1).

Defining the yielding settlement δ_y is slightly more complicated than the simple case with a single beam: the general procedure starts from the choice of the most stressed cross-section from the combination of vertical permanent loads and the imposed settlements. The definition of δ_y is then based on the ration between the residual bending capacity after the application of vertical loads and the bending moment generated by the unitary settlement pattern (0; 0,25; 0,5; 0,75; 1):

$$\delta_y = \frac{\left(M_{Rd} - {M_{Ed}}^{G_1+G_2}\right)}{{M_{Ed}}^{\delta=1}}$$

In this way when the load pattern $\delta = \delta_y$ is applied together with the permanent loads G1 and G2 the most stressed cross-section is subjected to an external bending moment $M_{Ed} = M_{Rd}$.

The value of δ_y for the first settlement configuration in the case of the "weak beam" structure is 4,83 cm, while in the case of "weak column" it is equal to 13,3 cm given the lower stiffness.

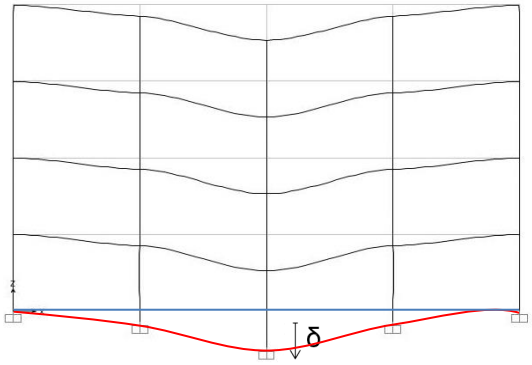

Figure 35 - settlement configuration 2

SETTLEMENT CONFIGURATION 2

The second settlement configuration is a symmetric settlement, following the pattern δ (0; 0,3; 1; 0,3; 0) as it is shown in Figure 35.

This settlement configuration is more demanding with respect to the previous one, given the fact that the differential settlements are larger from one

support to the adjacent one. The yielding parameter δ_y is thus 0,65 cm for the case of the "weak beam" and 1,4 cm for in the case of "weak column".

5.3 STATIC PLASTIC ANALYSIS (VERTICAL PUSH-OVER)

In order to evaluate the relationship between the bearing capacity of the structure and the initial settlements the ultimate load multiplier will be evaluated by means of a non-linear plastic analysis, performed increasing the vertical variable load multiplier λ_Q. The initial state of the structure is giving by the application of both the permanent loads G1 and G2 and the settlement ratio as:

$$\gamma_{G1} G_1 + \gamma_{G2} G_2 + \delta = 1{,}3\, G_1 + 1{,}5\, G_2 + \xi\, \delta_y \;\; ; \;\; \xi \in [0{,}1]$$

The variable load is then increased by means of the factor λ_Q until reaching the collapse.

5.3.1 CROSS-SECTION MODELS

In order to evaluate quantitatively the effect on ductility on the relation between the collapse load and the initial settlements different levels of cross-sectional ductility will be given to the elements and the structure will then be pushed to failure. In the end the critical or ultimate load multiplier will be function of both settlements and ductility levels:

$$\lambda_{CR} = \lambda_{CR}(\xi\, ;\, \mu)$$

In particular three levels are defined as reported in Figure 36:

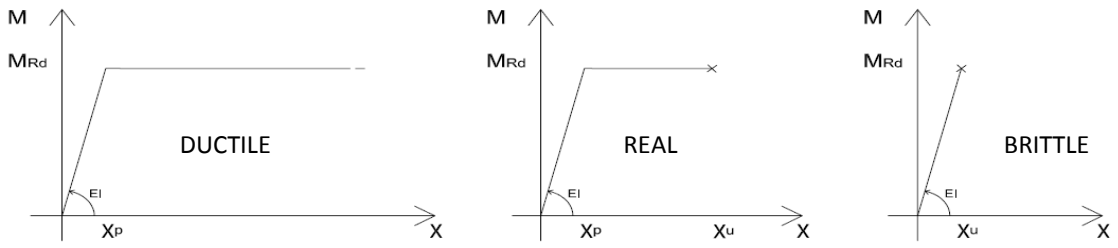

Figure 36 - cross-sectional ductility models

The cross-section in the "DUCTILE" case have a ductility that tends to infinite, while the "BRITTLE" cross-section fails as soon as the maximum capacity is reached.

In the case "REAL" the cross-section has a finite ductility, i.e. the ultimate condition is reached when the ultimate curvature is reached. In this case the plastic non-linear analysis can be still

performed but the maximum rotational capacity of the plastic hinges must be carefully defined. The rotation capacity of plastic hinges of reinforced concrete elements depends on many factors, therefore many different expressions are available, one of the most simple and widespread is the one proposed by Baker and Aramakone in 1964 for non-confined elements:

$\Theta_p = \frac{\varepsilon_{cu}-\varepsilon_{c,el}}{x_u} L_P$ for cracked sections

$\Theta_p = \frac{\varepsilon_{cu}-\varepsilon_{c,el}}{\mathrm{d}} L_P$ for fully-compressed elements.

Where:

- ε_{cu} and $\varepsilon_{c,el}$ are the plastic and elastic limit strains for concrete and value 3,5‰ and 2,0‰
- x_u is the position of neutral axis in ultimate conditions;
- L_P is the length of the plastic hinge evaluated as follows:

$$L_P = k_1 k_2 k_3 \left(\frac{\mathrm{z}}{d}\right)^{\frac{1}{4}} d$$

Where:

- $k_1 = 0{,}7$ for hot rolled steel bars;
- $k_2 = \left(1 + 0{,}5\frac{N}{N_{Rd}}\right)$ takes into account the normal force N;
- $k_3 = 0{,}78$ for concrete cubic resistance $R_{ck} = 30\ MPa$;
- z is the distance between the two section having the maximum ant the null bending moment;
- d is the distance between the reinforcement ant the top of the beam.

The parameters are reported in the following table:

	WEAK BEAM		**WEAK COLUMN**	
	BEAM 30X50	COLUMN30X60	BEAM30X50	COLUMN 40X40
h [cm]	50	60	50	40
b [cm]	30	30	30	40
d [cm]	46	56	46	36
M_{Rd} [kNm]	135	>135	210	<210
x_u [cm]	5,3	32	5,1	36
L_p [cm]	34,8	45,4	34,8	41,6
Θ_p [rad]	0,010	0,0024	0,099	0,0013

5.3.2 "WEAK BEAM" STRUCTURE

Given all the parameters described in the previous chapters, the vertical pushover analysis is performed increasing the parameter λ_Q until failure in the following load combination:

$$\gamma_{G1} G_1 + \gamma_{G2} G_2 + \xi \delta_y + \lambda_Q Q \quad ; \quad \xi \in [0,1]$$

The maximum load multiplier has been obtained with the ductile case, it is independent on the grade or the configuration of settlement and is:

$$\lambda_{Q,max}(\xi) = 3{,}07 \quad \forall \xi \in [0,1]$$

The value by itself is not of major interest and depends on the resistance of the elements and their geometry. It is interesting to compare this value with the ones obtained with the cases of lower ductility:

- in the case of "REAL" ductility the value appears again to be independent on the grade or the configuration of settlement and is $\lambda_{Q,max}(\xi) = 3{,}03 \quad \forall \xi \in [0,1]$;
- in the case of "BRITTLE" cross-sections, the value of $\lambda_{Q,max}$ is lower than 3,07 even for zero settlement, in fact it values 2,40; moreover it appears to be strictly dependent on the settlement grade ξ and tends to be zero for $\xi = 0$ as expected.

This results are summarized in the following graph, where $\lambda_{Q,max}(\xi)$ is reported for the three different levels of ductility and for the two settlement configurations.

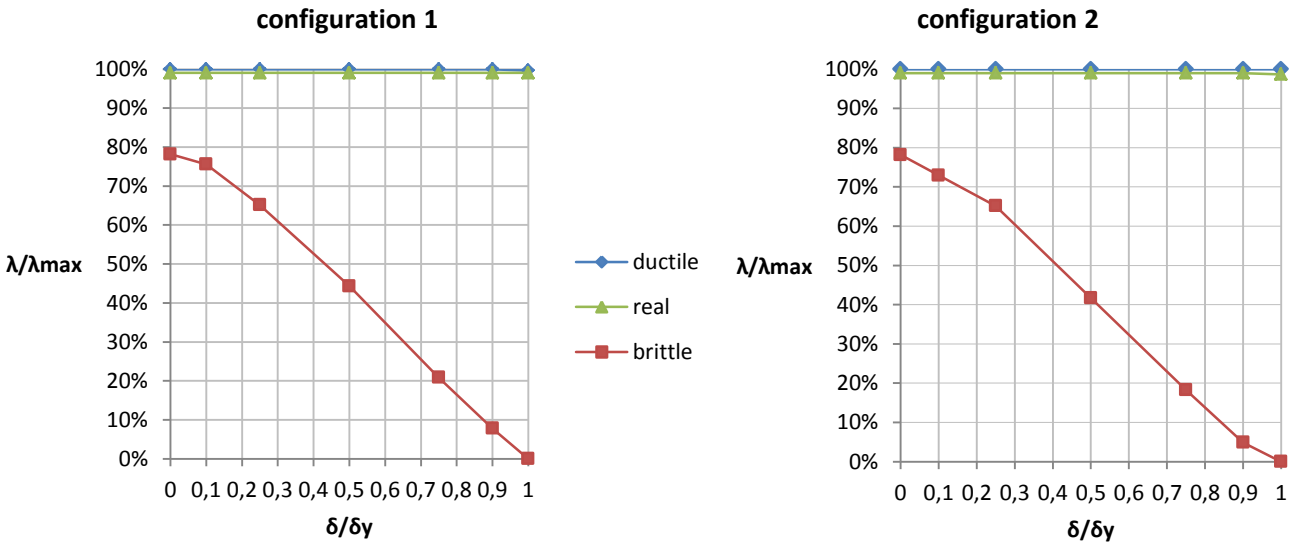

Figure 37 - ultimate capacity vs. degree of settlement

The results are also reported in the following tables:

λ_Q max						
ξ - conf 1	ductile		real		brittle	
0	3,07	100%	3,04	99%	2,40	78%
0,1	3,07	100%	3,04	99%	2,32	76%
0,25	3,07	100%	3,04	99%	2,00	65%
0,5	3,07	100%	3,04	99%	1,36	44%
0,75	3,07	100%	3,04	99%	0,64	21%
0,9	3,07	100%	3,04	99%	0,24	8%
1	3,06	100%	3,04	99%	0,00	0%

λ_Q max						
ξ - config 2	ductile		real		brittle	
0	3,07	100%	3,04	99%	2,40	78%
0,1	3,07	100%	3,04	99%	2,24	73%
0,25	3,07	100%	3,04	99%	2,00	65%
0,5	3,07	100%	3,04	99%	1,28	42%
0,75	3,07	100%	3,04	99%	0,56	18%
0,9	3,07	100%	3,04	99%	0,15	5%
1	3,06	100%	3,03	99%	0,00	0%

5.3.3 "WEAK COLUMN" STRUCTURE

The procedure for the "weak column" case is more complex as far as the resisting bending moment is function of the normal load applied:

$$M_{Rd} = M_{Rd}(N_{Ed})$$

This situation makes extremely complex and time consuming the definition of a yielding settlement δ_y for the two settlement configurations. This means that the value of δ_y may not correspond to the effective yielding condition of the most stressed element; nevertheless some data have been reported in order to find a correlation between some settlement grades $\frac{\delta}{\delta_y}$ the ultimate loads and the ductility levels of the cross-sections.

Moreover when the crisis is due to the columns the ductility of the "REAL" case is of complex definition but in general lower than the one provided by the column because it has to be remarked that the presence of normal force applied to the section reduces its flexural ductility.

The vertical pushover analysis is performed increasing the parameter λ_Q until failure in the following load combination: $\gamma_{G1}G_{\ 1} + \gamma_{G2}G_{\ 2} + \ \xi\ \delta_y + \lambda_Q Q \quad ; \quad \xi \in [0,1]$.

The maximum load multiplier has been obtained with the ductile case, it is independent on the grade or the configuration of settlement and is $\lambda_{Q,max}(\xi) = 4{,}7 \quad \forall \xi \in [0,1]$.

The value by itself is not of major interest and depends on the resistance of the elements and their geometry. It is interesting to compare this value with the ones obtained with the cases of lower ductility:

- in the case of "REAL" ductility the value is $\lambda_{Q,max}(\xi) = 3{,}54$;
- in the case of "BRITTLE" cross-sections, the value of $\lambda_{Q,max}$ is lower, for zero settlement it values 2,34 and in general decreases when ξ increases.

This results are summarized in the following graph, where $\lambda_{Q,max}(\xi)$ is reported for the three different levels of ductility and for the two settlement configurations.

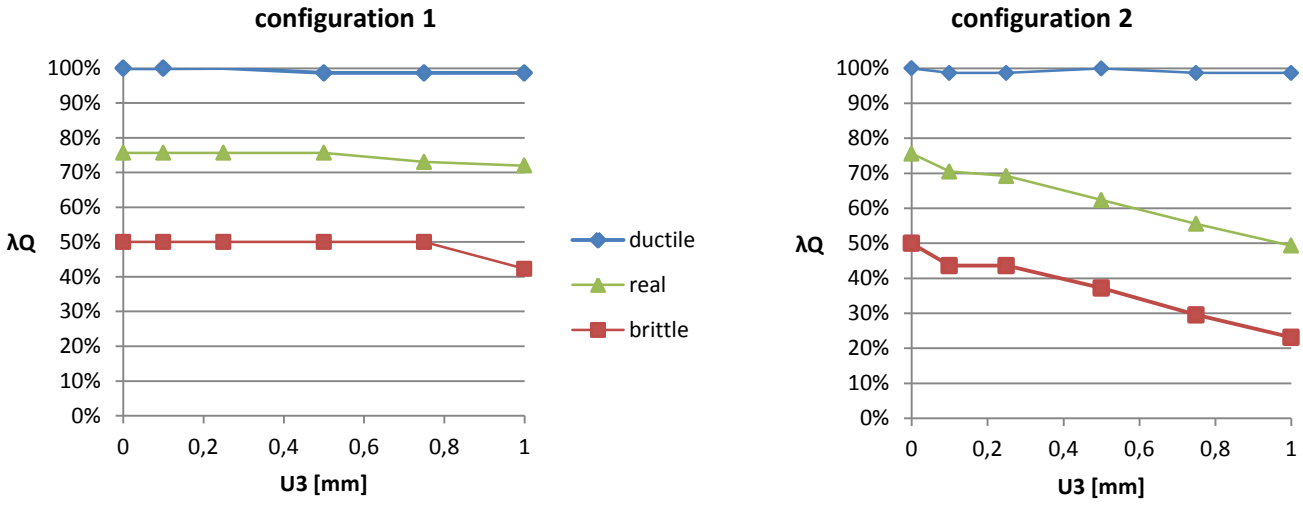

Figure 38 - ultimate capacity vs. settlement grad

The results are also reported in the following tables:

λ_Q max						
ξ - conf 1	ductile		real		brittle	
0	4,7	100%	3,54	76%	2,34	50%
0,1	4,7	100%	3,54	76%	2,34	50%
0,25	4,7	100%	3,54	76%	2,34	50%
0,5	4,6	99%	3,54	76%	2,34	50%
0,75	4,6	99%	3,42	73%	2,34	50%
1	4,6	99%	3,37	72%	1,98	42%

λ_Q max						
ξ - conf 2	ductile		real		brittle	
0	4,7	100%	3,54	76%	2,34	50%
0,1	4,6	99%	3,3	70%	2,04	44%
0,25	4,6	99%	3,24	69%	2,04	44%
0,5	4,7	100%	2,92	62%	1,74	37%
0,75	4,6	99%	2,6	56%	1,38	30%
1	4,6	99%	2,31	49%	1,08	23%

5.4 CONCLUSIONS

Given the previous results some remarks are possible:

- in all the previous cases the resistance of elements is not changed, the only variable parameters are the elements ductility and the initial settlements imposed to the frames
- in the case of "weak beam" the behaviour of the structure is largely expected, i.e. the bearing capacity of brittle structure is reasonably lower and strictly dependent on the settlement grade, no difference is registered between the two settlement configurations. On the other hand the "ductile" and the "real" structures resistance is not dependent at all on the settlement grade and appears to be really similar, this is due to the fact that failure happens in the beam, in which the effective ductility is really large and independent on the loads applied.

- in the case of “weak column” the results are less expected but for this reason more interesting. In first instance the brittle structures resistance do not show a strict dependence on the settlement grade as in the case of “weak beam” but show a general decrease; this may be addressed to the fact that especially with lower settlement degrees ($\xi = 0 \div 0{,}5$) failure happens in cross-section poorly stressed by the initial settlements. In fact failure appears in the last storey columns, while the settlement of supports causes the most strong effects on the first storey columns as shown in Figure 39 .

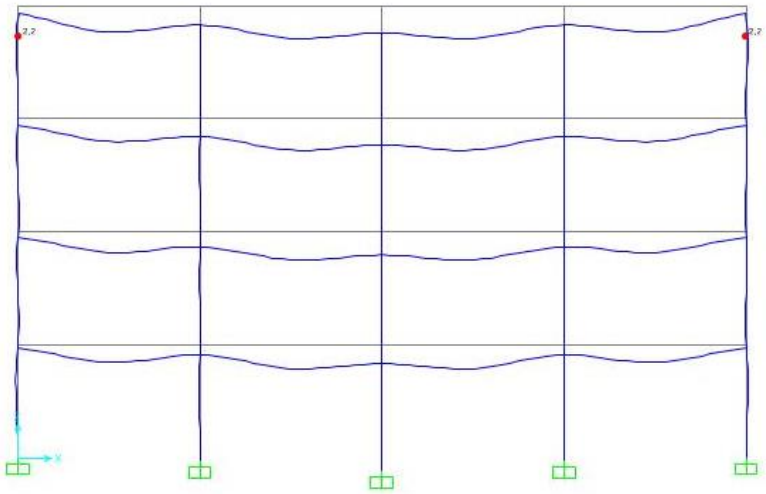

Figure 39 - brittle failure in "weak column" case

Moreover in the case of “real” ductility the bearing capacity decreases strongly with respect to the “weak beam” case, this is due to the fact that the ductility of a compressed column is much lower than the one of the beam due to the very low position of the neutral axis at the ultimate condition. The “ductile” structure indeed show an higher bearing capacity and a total insensivity to the settlements conditions.

In conclusion of this chapter it is possible to notice the double benefit that ductility provides to structures: the ductile structures with equal resisting bending moment are able of an higher bearing capacity given the possibility to develop a plastic failure mechanism; moreover the ductile structures show the possibility to “adapt” to imperfection that cause initial coercive states without any lost in the ultimate load bearing capacity.

It has to be reported that, as it happened in the case of “weak column”, failure may be not fully dependent on the initial coercive states even for brittle structures. In this case the linear-elastic analysis of the structure is very useful to understand the internal forces distribution at low load levels in order to understand the effective correlation between settlements and failure modes of the structure.

6. PORTOMAGGIORE STUDY CASE

6.1 INTRODUCTION

All the ideas described in the previous chapters will be now applied to a real structure. The study case concerns a collapsed covering of a sports hall of the school campus of Portomaggiore, province of Ferrara (Emilia Romagna, Italy).

Figure 40 - Portomaggiore gym

The gym is a recent building, construction works started in 2005 and finished in March 2008. After only two years in service, the roof collapsed on 10th March 2010 in the early hours of the day. The external cause was an overload due to an ordinary snowfall. As it will be explained in the following chapters, the failure was caused by the junction system of the spatial steel truss that formed the covering system, as far as it does not provide enough strength and ductility.

In order to evaluate the effect of ductility on the ultimate load, different levels of ductility and strength will be given to the resisting truss structure, starting from theoretical values and approaching gradually the real behaviour of trusses at the moment of collapse; all the related maximum snow load will be then reported and compared in case of different initial coercive states.

6.1.1 DESCRIPTION OF THE STRUCTURE

The building is a prismatic structure, the dimensions are approximately 43x27 meters in plan and 9,8 m in elevation. In the following description two systems will be defined, the first is the concrete frame system, it has the function of transmitting the vertical loads from the roof to the foundations and is also the horizontal resisting system. The second system is the steel truss

system composing the cover of the sports hall; as it will be exposed in the following, the causes of collapse concern almost exclusively this second structure.

CONCRETE FRAME

The frame system is composed of twenty concrete pillars, (60x50 cm of section), giving height to the copping beam (50x85 cm of section). The copping concrete beam has a regular span of 6,55 meters on the short side and 7,03 meters on the long one. The foundation system is a strip footing, supporting the twenty columns and forming a regular grid on the interior of the structure on order to give a larger regularity to the system.

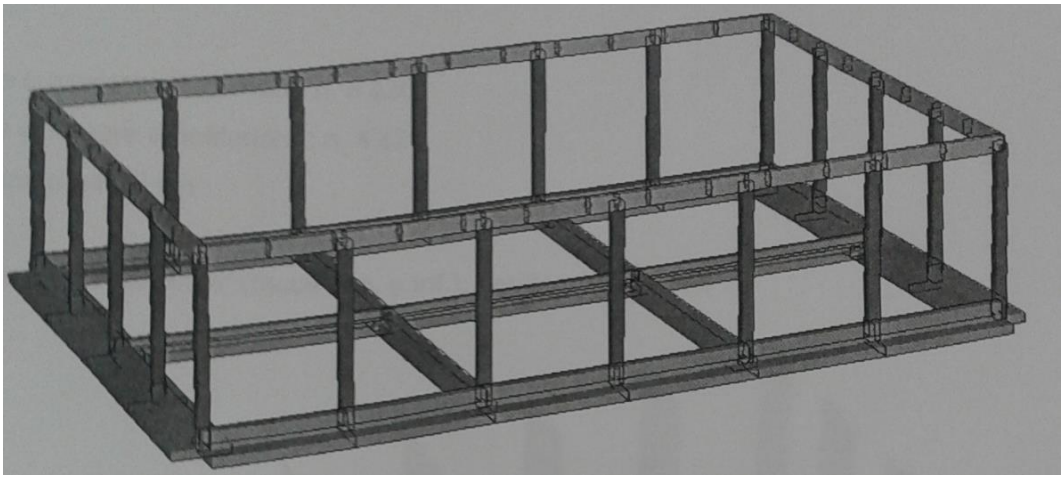

Figure 41 - Concrete frame system with foundations

This structure did not suffer almost any damage during collapse and was not involved in the failure. In the following table are reported the mechanical parameters of the reinforced concrete, as described in the design technical report:

Foundations concrete	Class R_{ck}=30 N/mm^2
Frame concrete	Class R_{ck}=35 N/mm^2
Steel reebars	Class FeB44K

STEEL TRUSS ROOF

The truss system supporting the sports hall cover is composed of 790 rods, divided into two layers, each one counts 187 rods, the lower ones work mainly under traction while the upper ones are subjected to compression.

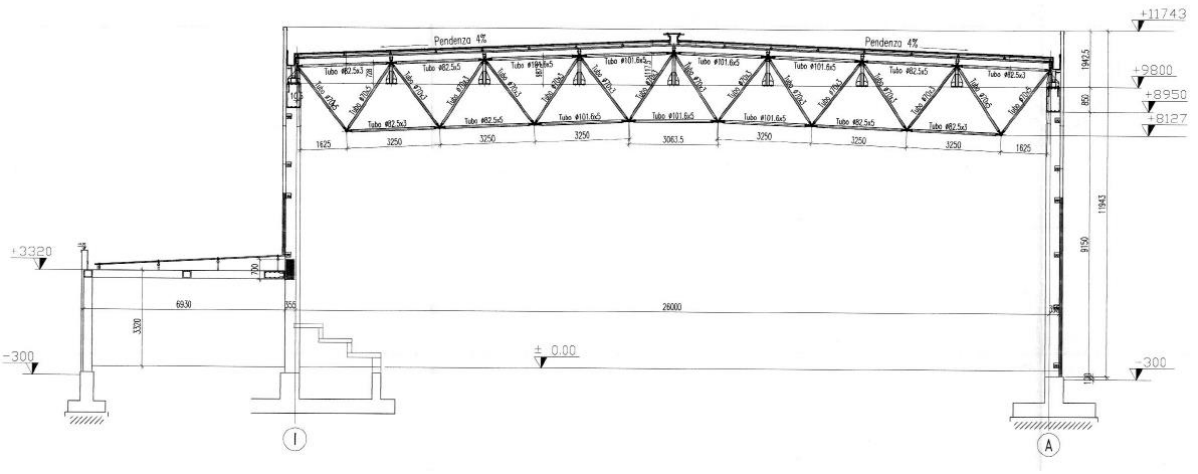

Figure 42 - steel truss elevation

The two layers are connected by 416 diagonal rods to guarantee shear connection. All components are 3,25 meters long, i.e. the truss system is composed of equilateral pyramids. The two layers are thus 2,30 meters far from each other. All rods are connected by 230 nodes, made of a screw and spheres system. The steel truss system transfers the loads to the concrete frame through 42 steel supports. In the middle of the lower layer, the central rod is shorter (3,00 meters) in order to give to the roof a 4% slope in the transversal or shorter direction for rain water discharge.

6.1.2 TRUSS SYSTEM DESCRIPTION

The only part of the structure that was involved in the collapse on the 10th March 2010 was the truss system, in the following chapter all its components will be shortly described.

RODS

The rods are made of structural steel S275 JR, characterized by a yielding stress of 275 N/mm^2, an ultimate stress of 430 N/mm^2, modulus of elasticity of 210 GPa.

All the rods have a tubular cross-section, defined in the following lines by its external diameter and its thickness denoted by the code B_diameter X thickness. Five different cross-sections are present in the steel truss: B70x3 and B70x5 for the diagonals and B82.5x3; B82.5x5, B101.6x5 for the horizontal layers. In the following table all the relevant cross-sectional parameters are reported:

SECTION	m [kg/m]	A_s [cm]	I [cm^4]	ρ	W_{el} [cm^3]	N_{Rd}^{+} $[kN]$	$N_{cr,e}^{-}$ $[kN]$	N_{buck}^{+} $[kN]$
B70x3	5,0	6,3	35,5	2,4	10,1	165	-68	-56
B70x5	8,0	10,2	54,2	2,3	15,5	267	-104	-85
B82.5x3	5,9	7,5	59,3	2,8	14,4	196	-114	-88
B82.5x5	9,6	12,2	91,8	2,8	22,3	319	-177	-139
B101.6x5	11,9	15,2	177,0	3,4	34,9	397	-342	-235

Where:

- m is the self-weight expressed in [kg/m];
- As is the cross-sectional area
- I is the moment of inertia of the cross-section in every direction given the circular shape;
- $\rho = \sqrt{I/A}$ is the radius of gyration of the section;
- W_{el} is the elastic modulus of the section;
- N_{Rd}^{+} is the yielding tension axial force;
- $N_{cr,e}^{-}$ is the eulerian critical load taking the free length $l_0 = l = 3{,}25\ m$;
- N_{buck}^{+} is the buckling load given by the Italian standard[6].

[6] NTC08 , cap 4.2.4.1.3 ,curve a

CONNECTION SYSTEM

The connection system is composed of a large number of elements connecting each rod to the others, in each connection point meet in average eight rods connected by a system of screws to a single sphere. The series of components is depicted in Figure 43:

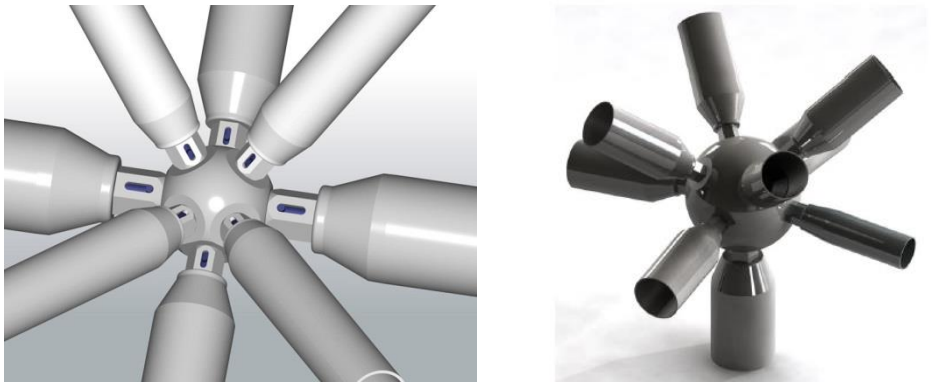

Figure 43 - 'Mero kk' connection system

These connections are similar to the type 'Mero kk' as the German company MERO TSK Gmbh patented these joints at the 40's.

The connection system is compound of 5 pieces: 'Sfera-stress', 'Vite-stress', 'Ghiera-stress', 'Nottolino-stress' and 'Terminale-stress'. In the next lines it will be explained the function of each piece.

- **'Sfera-stress'**: all the rods axis converge in the central point where the sphere is placed. The material of the spheres is a non-alloy free-cutting steel according to the norm EN 10027-1, table 13. It is similar to steel 11SMnPb37 which properties are specified in the norms EN 10087 and EN 10277-3. The main properties are the yielding stress f_y = 375 MPa and the tensile strength f_u = 460 MPa. The designer took an admissible strength σ_{adm} = 250 MPa.
- **'Vite-stress'**: it is the adjacent element to the sphere. It's a fastener with two different screws, the big one, screwed to the element 'ghiera-stress' and the small one festende to the 'sphere-stress'. They are the transition between a small screw suitable to the small drill made in the sphere and the conic piece called 'ghiera-stress'. The 'vite-stress' is made of a non-alloy steel according to the norm EN 10027-1, table 12, similar to a steel C60 which properties are specified in the norms EN 10083 and EN 10277-2. The main properties are the yielding stress f_y = 780 MPa and the tensile strength f_u = 930 MPa. The designer took an allowable stress σ_{adm} = 520 MPa.

- **‘Ghiera-stress’** : it is the conic elements which makes the transition between a small screw and the diameter of the rod in order to connect through the ‘terminale-stress’ the rod. It is made of the same material of ‘sfera-stress’, that is the steel 11SMnPb37.
- ‘**Nottolino-stress’** : It’s a special kind of bolt, also called stud, i.e. a bold without head where all the shank is threaded in order to connect two female screws composing the ‘ghiera-stress’ and the ‘terminale stress’. The material of the ‘nottolino-stress’ is specified fastener which properties are regulated by ISO norm 898-1. The normalized class of the stud is 10.9 with the following properties: yielding stress f_y = 900 MPa and the tensile strength f_u = 1000 MPa. The designer took an admissible stress of σ_{adm} = 458 MPa.
- **‘Terminale-stress’** : It’s the last element of the linking system and it has a female screw to join the ‘nottolino-stress’ in one side and in the other one is welded with the rod. It is made of the same material of the ‘sfera-stress’, that is the steel 11SMnPb37.

In the next picture the position of each component is depicted.

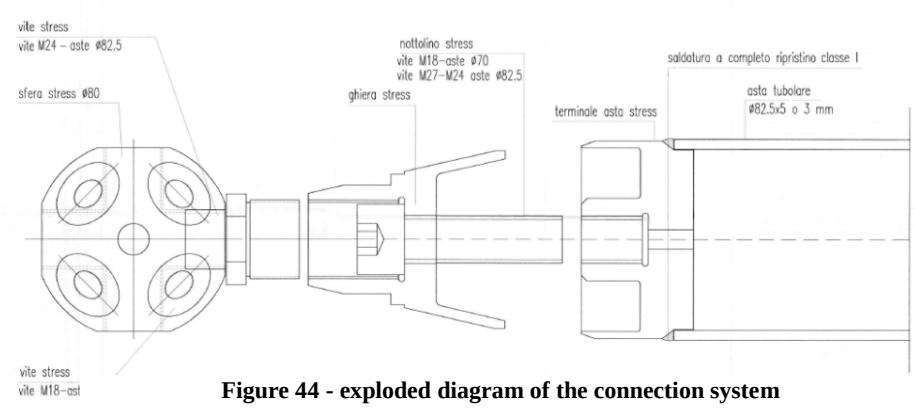

Figure 44 - exploded diagram of the connection system

SUPPORTS

The truss system is connected to the concrete frame by means of 42 steel supports. This connectors are made of a vertical steel rod welded steel plates and ribs in order to abstain a stiff element. The supports are then connected to the concrete girder by means of ISO bolts M22 drowned in concrete at the moment of cast and then inserted into the holes of the base plate of the supports and tighten with a nut. The rod is then screwed to the first ‘Sfera-stress’ of the truss system.

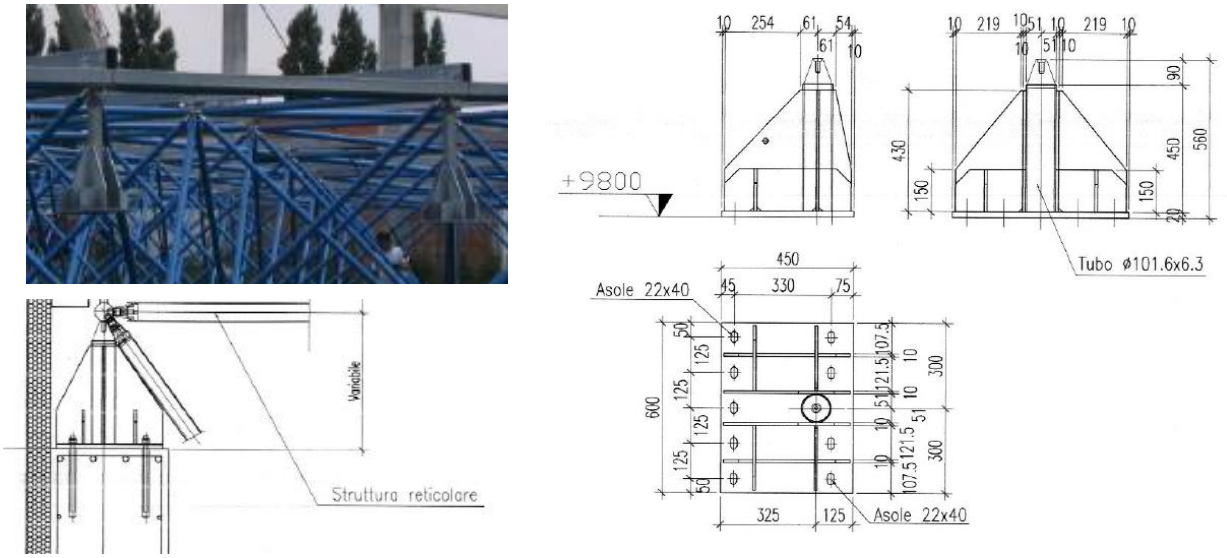

Figure 45 - steel supports

TRACTION TESTS ON THE CONNECTION SYSTEM

In the framework of this thesis the ultimate load bearing capacity of the structure has to be compared between different levels of ductility and initial imperfections:

$$q_U = q_U\,(\xi\,;\,\mu)$$

The main cause of the collapse on the 10th March 2010 was the bad quality of the connection system, in particular in the thread between the components "sfera-stress" and "vite-stress", which led to a strong decrease in both resistance and ductility of the connection. The aim of this thesis does not regard the particular failure mechanism of the screwed system or the material quality, the only two relevant parameters taken into account are the connection resistance and its ductility. Therefor in the following line are reported some results of the traction tests performed on the connection systems and the sections that are connected by each of them.

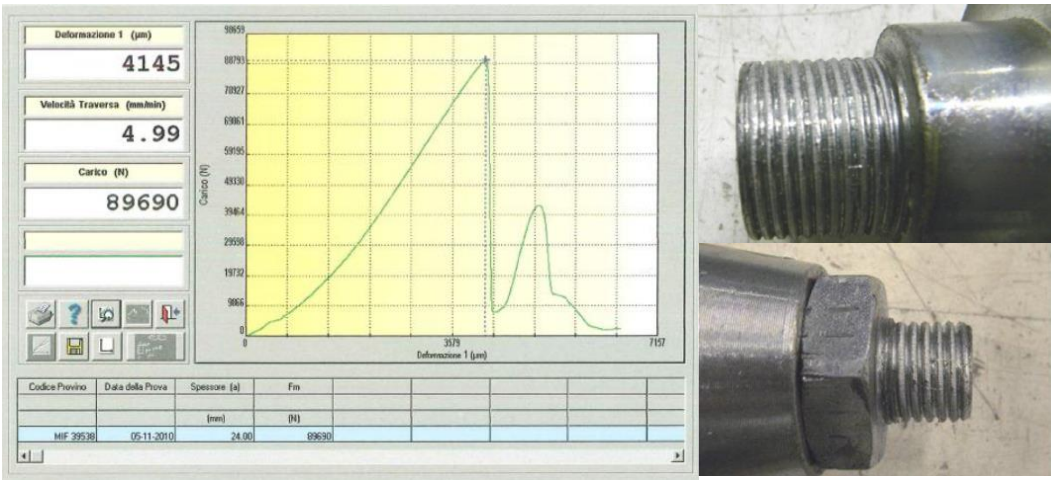

Figure 46 - traction tests on the connection system

The traction tests show a strongly brittle behaviour of the connection that fails suddenly for the pull-out of the "vite-stress" from the "sfera-stress". The pull-out happens with the reduction of the external diameter of the bolt of "vite-stress" and the internal diameter of "sfera-stress" as shown in Figure 46 The values for the different types of connections are reported in the following table:

BOLT	A [mm^2]	σ_{adm} [N/mm^2]	N_{Rd}^{EXP} $[kN]$	N_{Rd}^{REAL} $[kN]$	RODS CONNECTED
M30	561	520	291,7	227,7	B101.6x5
M24	353	520	183,6	89,7	B82.5x3 & B82.5x5
M18	192	520	99,8	83,3÷80,8	B70x3 & B70x5

Where:

- A is the area of nominal effort for each bolt section

- σ_{adm} is the admissible stress defined by the designer for the material composing the bolts, similar to a steel C60;

- N_{Rd}^{EXP} is the expected exercise force of the connections;

- N_{Rd}^{REAL} is the maximum traction force obtained from the tests

- RODS CONNECTED indicates which cross-sections are connected by the different types of "vite stress".

6.2 ACTIONS

In the following paragraphs all the loads applied to the model are reported.

6.2.1 PERMANENT LOADS

The permanent loads applied to the truss system are given by the only self-weight of the steel structure and the permanent non-structural components of the cover and insulation layers.

The self-weight of the steel components obtained by the steel density ($\rho_s = 7{,}85\ {}^{t}/_{m^3}$) is approximately $G_{1,k} \cong 16\ {}^{kg}/_{m^2}$ on the roof surface.

The permanent non-structural load has been evaluated by the designer as $G_{2,k} = 25\ {}^{kg}/_{m^2}$.

This load expressed as a distributed load has been applied to the truss model as concentrated forces on the upper layer nodes, given the influence area $A_{G2} = 3{,}25 \times 3{,}25\ m^2 = 10{,}56\ m^2$. To all the nodes of the upper layer have been thus applied 2,65 kN .

6.2.2 VARIABLE LOADS

The loads described in the following paragraph are denominated "variable" not only because of their nature, as for the snow load, but rather because both the snow load and the initial supports displacements are varied in order to obtain the maximum snow load bearing capacity as a function of the initial imperfection generated by the initial supports displacements.

Q – SNOW LOAD

The snow load indicated by the designer is equal to a distributed load $Q_k = 160 \times 0{,}8 = 128\ {}^{kg}/_{m^2}$ The engineer that investigated on this case reported that in the night of the 10th March 2010 the actual snow load was considerably lower, evaluated as $Q_{collapse} = 40\ {}^{kg}/_{m^2}$, approximately one third of the characteristic expected value.

SUPPORTS DISPLACEMENTS

The supports initial displacements have been defined as a random extraction of 42 values from a normal distribution having average μ=0 mm and a standard deviation of $\sigma = \frac{5\ mm}{1{,}64} = 3{,}05\ mm$ defined in order to obtain the 95th percentile equal to 5 millimetres. the next figure shows the displacement application on the 42 supports reported in millimetres.

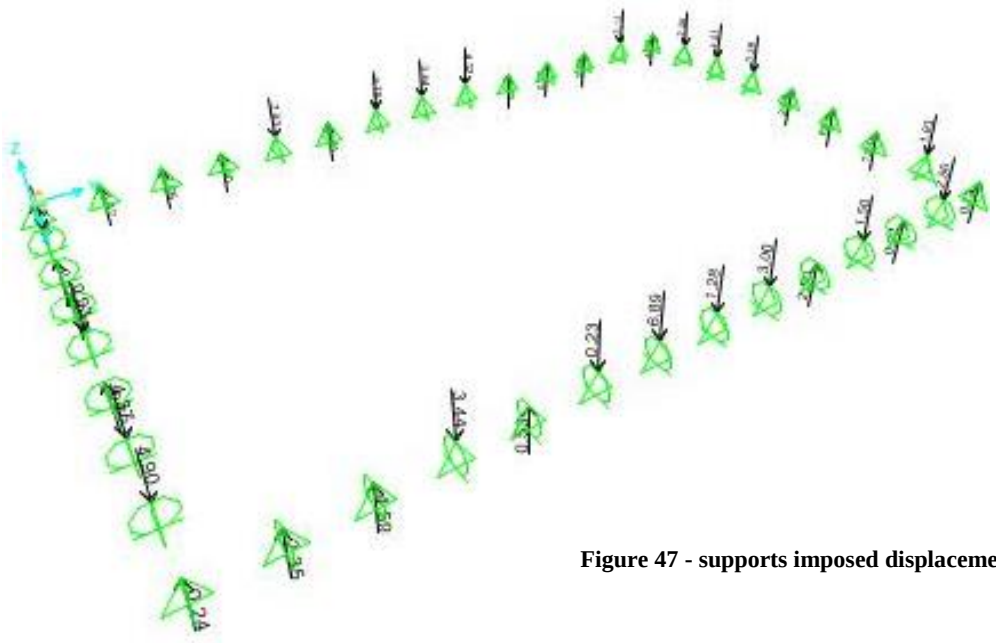

Figure 47 - supports imposed displacements

6.3 STRUCTURAL ANALYSYS

In order to understand the magnitude of the actions applied to the elements and the required structural performance, some linear elastic analysis have been performed on the structural model. The linear load combinations applied to the structure are:

- ULS: the ultimate vertical limit state evaluated as $\gamma_{G1}G_{1,k} + \gamma_{G2}G_{2,k} + \gamma_Q Q_k$
- Characteristic load combination : $G_{1,k} + G_{2,k} + Q_k$
- "collapse" load combination, i.e. the evaluated expected loads present on the structure at the moment of collapse : $G_{1,k} + G_{2,k} + Q_{collapse}$

6.3.1 LINEAR ELASTIC ANALYSYS

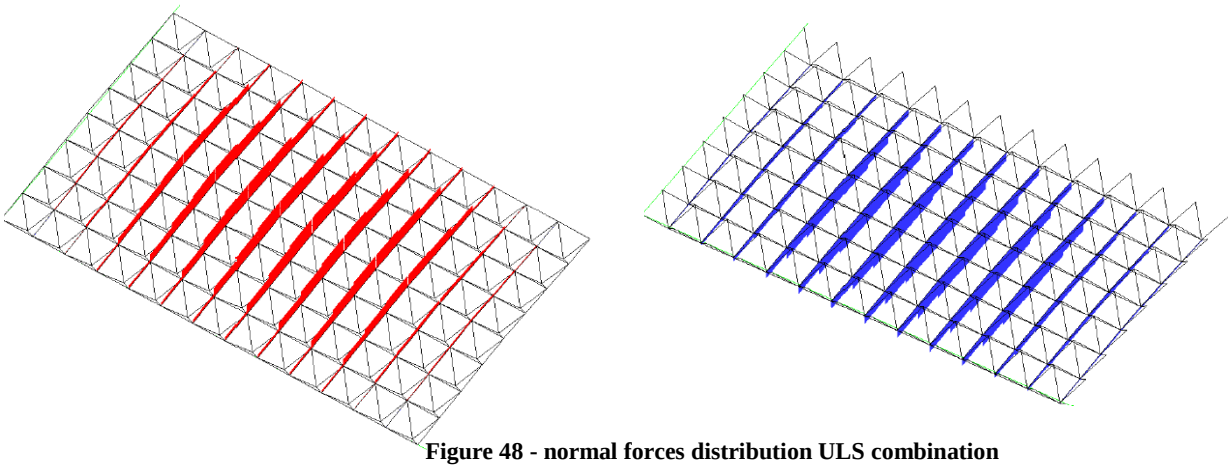

Figure 48 - normal forces distribution ULS combination

Given its rectangular shape, the truss system is divided into two main directions, a longitudinal one on the longest side of 42 meters and the shortest one 26 meters long. The horizontal rods are

following these two directions, the transversal alignment is the shorter, and thus the stiffer, that means the most stressed one; for this reason the transversal rods have the larger sections in the central position. The longitudinal rods on the contrary are less stressed and maintain the section B82.5x3 for the whole length. If the truss system is seen as a single component, the stresses in the horizontal rods follow the bending moment applied by the vertical load, that is larger in the central portion and decreases towards the supports as shown in Figure 48.

On the other hand the diagonal rods are stressed proportionally to the shear applied to the truss system as a whole. As shown in Figure 49, this means that the most stressed diagonal components are the ones placed towards the supports, their cross-sections are therefore larger, B70x3 in the central portions and B70x5 in the rods close to the supports.

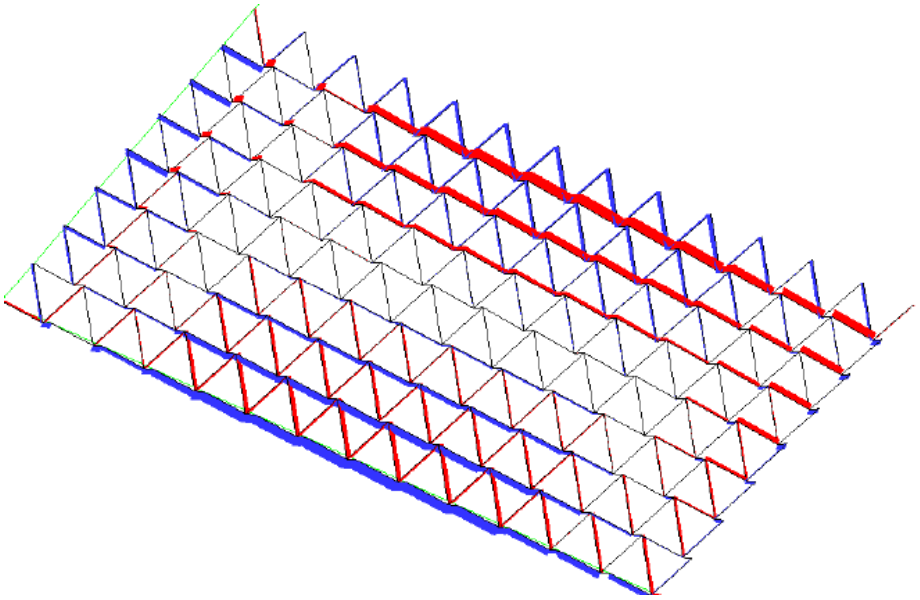

Figure 49 - normal forces distribution on diagonal rods ULS combination

In the ultimate limit state ULS combination the central rods of the upper transversal layer, section B101,6x5, are subjected to a maximum of 260 kN compression force, in the longitudinal direction, section B82,5x3, to a maximum of 90 kN in compression. In the lower layer in the transversal direction the most stressed rods with a section of B101,6x5 are subjected to 250 kN under traction, while in the longitudinal direction with a section B82,5x3, the most stressed rods are subjected to only 80 kN under traction.

6.3.2 BUCKLING ANALYSIS & VERIFICATIONS

As far as the rods composing the truss system are very slender, the buckling resistance is the real resistance of rods under compression. In the composition of the truss system all the elements subjected to compression have the same length (3,25 m); given that the rotational stiffness of the connection system is really difficult to evaluate and modelling the truss system as connected by hinges, the effective length is taken as $l_0 = l = 3{,}25\ m$. In the following table all the buckling resisting forces of the different cross-section are reported:

section	$N_{Rd}^{+}\ [kN]$	L_0 [m]	A [m2]	I [m4]	ρ [m]	λ
70x3	**165**	3,25	0,000631	3,55E-07	0,024	137
70x5	**267**	3,25	0,001021	5,42E-07	0,023	141
82,5x3	**196**	3,25	0,000749	5,93E-07	0,028	116
82,5x5	**319**	3,25	0,001217	9,18E-07	0,027	118
101x5	**397**	3,25	0,001517	1,78E-06	0,034	95
	NTC 08					
section	α - curve a	$N_{cr,e}^{-}\ [kN]$	λ_	Φ	χ	$N_{buck}^{+}\ [kN]$
70x3	0,21	68,33	1,594	1,91603	0,335585	**55**
70x5	0,21	104,40	1,640	1,995838	0,319141	**85**
82,5x3	0,21	114,11	1,344	1,522632	0,446613	**88**
82,5x5	0,21	176,66	1,376	1,570727	0,429638	**137**
101x5	0,21	341,66	1,105	1,20553	0,592594	**235**

Where:

- N_{Rd}^{+} is the yielding tensile force
- L_0 , A , I are the effective length, cross-sectional area and inertial modulus
- $\rho = \sqrt{I/A}$ is the radius of gyration of the section;
- $\lambda = \rho/L$ is the elements slenderness;
- α is the imperfection factor given by Italian standards;
- $N_{cr,e}^{-}$ is the eulerian critical load;

Given these values some rods in the central portion appear to not be verified against buckling. This fact, even if relevant in the design process is not related to the collapse, that happened to lower force levels: the equivalent snow load for the ultimate limit state is approximately 207 kg/m^2, while the snow present at the moment of collapse was evaluated to be 40 kg/m^2.

A linear buckling analysis has also been performed in order to check the previously reported results and the buckling mode shapes and buckling load multiplier agreed fully.

6.4 STATIC PLASTIC ANALYSIS (PUSH-OVER)

In the framework of this thesis, a vertical push-over analysis has been performed on the numerical model in order to evaluate the structural ultimate capacity and the its relation with the initial imperfection describe in the paragraph 6.2.2. In order to investigate how this relation is influenced by the ductility, in the non-linear static analysis different cross-sectional model have been defined and then the ultimate snow load bearing capacity is been computed and compared.

6.4.1 CROSS-SECTION MODELS

The three cross-sectional force-displacement models relay on imposing to the members three different failure modes that influence both resistance and ductility of members.

YIELDING-YIELDING MECHANISM – STOCKY ELEMENTS

The firs model relies on the only material capacity, without taking into account any second-order effects or the connection capacity. The only failure possible for elements is yielding f the cross-section both in tension and compression as reported in the following graph:

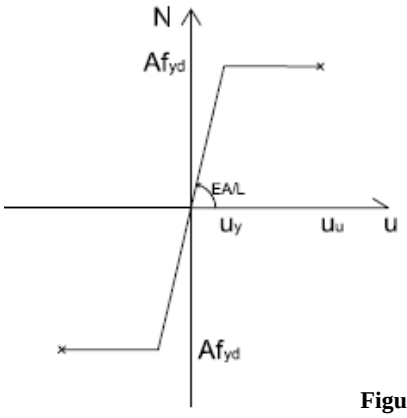

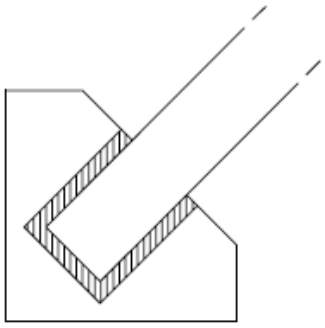

section	$N_{Rd}^{\mp}$ $[kN]$
70x3	∓165
70x5	∓267
82,5x3	∓196
82,5x5	∓319
101x5	∓397

Figure 50 - stocky elements model

As far as the failure mode is under compression only, in the abscissa the nodal displacement u is reported, it is related to the axial strain ε_z by the relation $u = \varepsilon_z\, L$.

Beside the graph is reported a sketch representing the rod element as stocky and connected by welding to the node, i.e. that exploits exactly the yielding force both in tension and in compression.

BUCKLING-YIELDING FAILURE MODE – SLENDER ELEMENTS

A second axial force-displacement model is defined taking into account the second order effects,. i.e. the buckling resistance of elements, but still considering the yielding resistance of the material under traction.

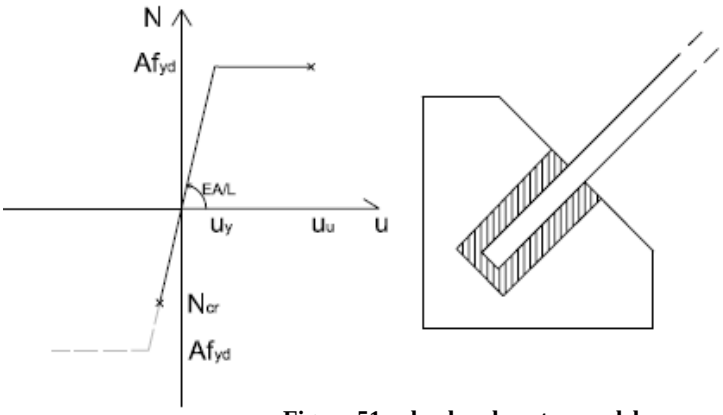

section	N_{Rd}^{+} $[kN]$	$N_{Rd,buck}^{-}$ $[kN$
70x3	165	-55
70x5	267	-85
82,5x3	196	-88
82,5x5	319	-137
101x5	397	-235

Figure 51 - slender elemetns model

BUCKLING-PULL-OUT FAILURE MODE – SLENDER ELEMENTS WITH CONNECTORS

The third force-displacement model takes into account also the connectors capacity under traction, while in compression the failure is given by buckling of the rods.

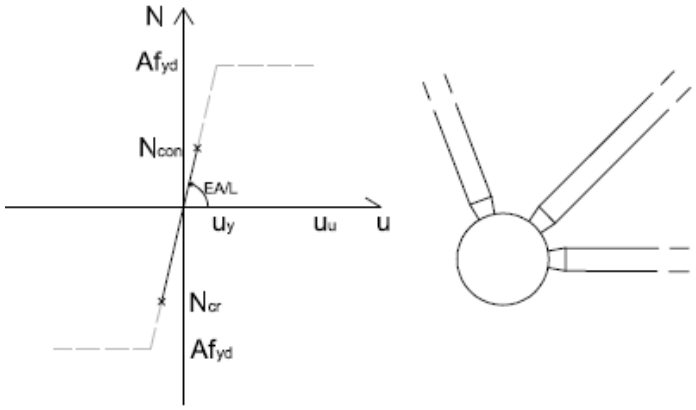

section	N_{conn}^{+} $[kN]$	$N_{Rd,buck}^{-}$ $[kN$
70x3	82,5	-55
70x5	82,5	-85
82,5x3	89,7	-88
82,5x5	89,7	-137
101x5	227,7	-235

Figure 52 - connected elements model

The connection capacity under traction is defined following the traction tests described in the paragraph 6.1.2 and the correspondence between connection systems and elements sections. When an element is connected to two different “vite-stress” systems, with different resistances, the weakest one is taken for the whole element.

SOFTWARE MODEL IMPLEMENTATION

In order to represent the models described in the previous paragraphs in the software different types of axial plastic hinges have been defined:

- For the "stocky-elements" model, the so called displacement-controlled plastic hinges have been defined, i.e. ductile hinges. These devices, put at the extremities of the element, start working as axial plastic hinges at the ends of elements when the yielding capacity is reached and maintain the same force level for the whole plastic deformation, until the ultimate strain ε_U is reached.
- In the "slender-elements" model, given the fact that the behaviour under traction is ductile and under compression is strongly brittle, the analysis was carried out "by hand": an incremental analysis has been performed making use of a Matlab code in order to manage the huge number of rods, extract the most stressed ones and if failed under traction, to remove them and to apply the further load increments until failure of the structure is reached.
- In the "slender-elements with connectors" model a software-based analysis has been carried out, making use of the so called force-controlled hinges, that correspond to the brittle failure modes given by buckling und pulling-out of the rods.

6.4.2 “STOCKY-ELEMENTS” STRUCTURE

The vertical pushover analysis is performed using as initial condition the presence of permanent loads with their characteristic value and the possible presence of supports settlement.

$$G_1 + G_2(+\delta)$$

The snow load is then increased until reaching failure of the steel truss. In this firs case the structure performs very well and huge ultimate snow load have been reached. In the following graph the snow load vs. the related central node deflection is reported.

On the graph the required snow load are reported for the ultimate limit state in blue, the characteristic combination in green and the snow load level present ate moment of collapse on the 10th March 2010 in red. The structure behaves linearly, i.e. no yielding of elements appears,

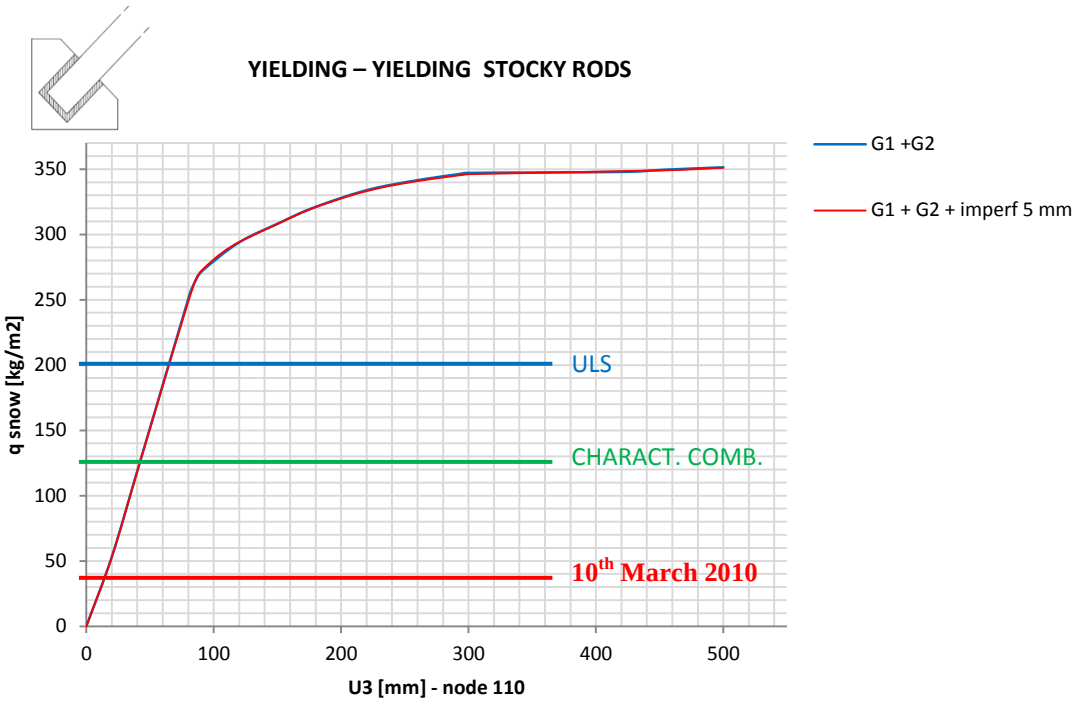

Figure 53 - force-displacemente graph

until the load of 265 kg/m^2, which is really beyond the 208 required by the ultimate limit state. Moreover the plastic benefit of the structure is very high: the ultimate snow loadbearing capacity of the structure taking into account the only yielding of its elements is 350 kg/m^2.

In the framework of the thesis, the influence of initial displacements of supports is evaluated: in the case of stocky-elements model the structural behaviour are strongly ductile, and no difference in the ultimate bearing capacity appears if initial supports settlements are given (red graph indicated as G1+G2+imperf 5mm).

6.4.3 “SLENDER-ELEMENTS” STRUCTURE

The overall bearing capacity of the structure decreases significantly if the buckling of the elements is taken into account. The two drawbacks that the second order effects imply are both a reduction on strength and the reduction of ductility under compression as far as buckling is a strongly brittle failure. in the following graph the snow load and the central deflection are reported.

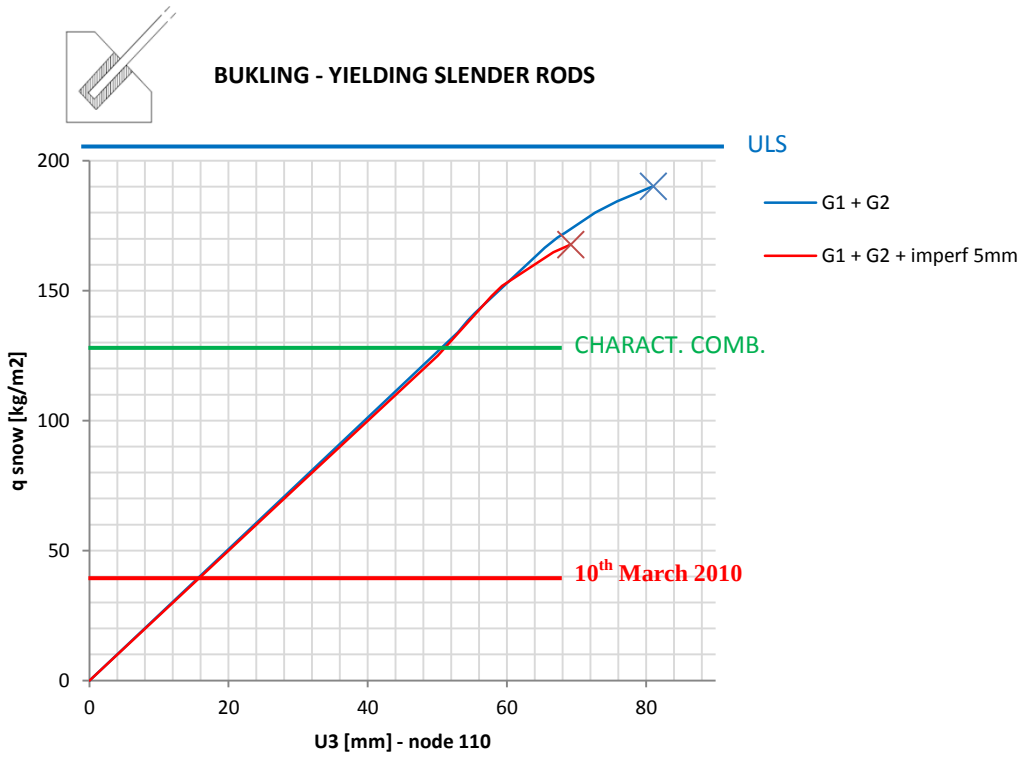

Figure 54 - force-displacement graph

In this second case the lower structural ductility and resistance are evident: the ultimate bearing capacity drops from the 350 to the 190 kg/m^2, and the ultimate deflection in the central node is only 8 cm. the first linear-elastic branch maintains the same slope, this means that the stiffness is not affected for lower loading levels.

The structural ductility is much lower given the brittleness of the buckling failure mode. This becomes more clear comparing different initial conditions: in the case of zero initial settlements with the only permanent loads applied (blue graph) the bearing capacity reaches 190 kg/m^2, while with the presence of the initial displacement distribution with the 95th percentile equal to 5 mm the ultimate capacity of the structure is only 155 kg/m^2.

It is interesting to notice how the fact that some rods are not verified against buckling is shown in the graph: the structure, even if in perfect conditions, cannot reach the ULS load level of 207 kg/m^2 (blue line).

6.4.4 "SLENDER ELEMENTS WITH CONNECTORS" STRUCTURE

Taking into account the traction resistance of connectors leads to a significant drop in the load-bearing capacity of the structure.

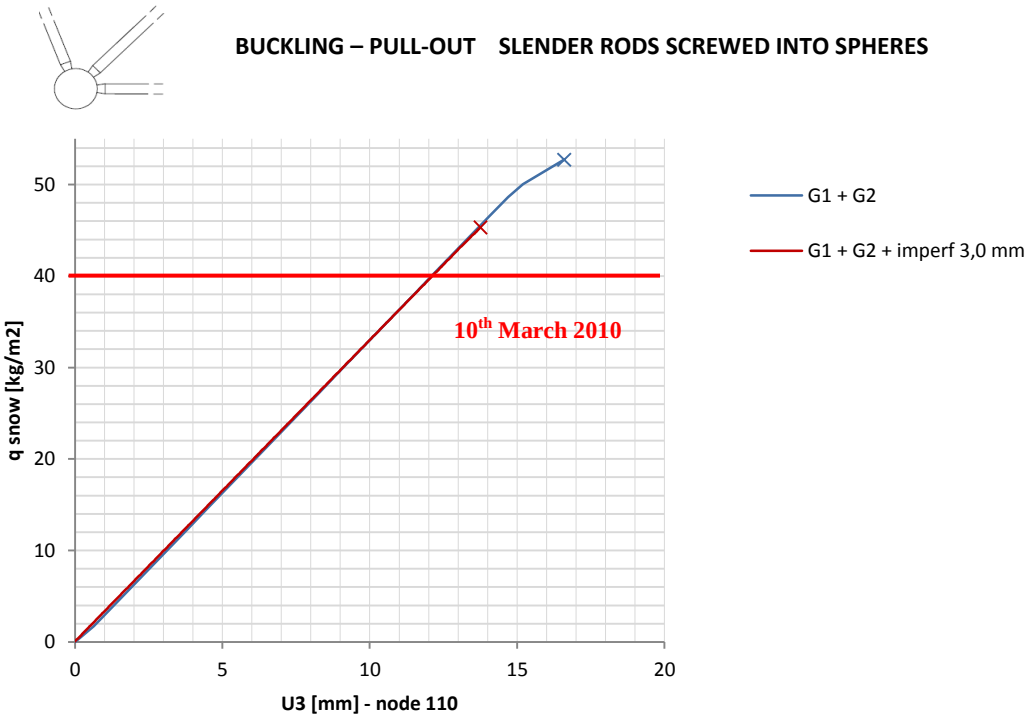

Figure 55 - force-displacement graph

The overall capacity is decreased to 53 kg/m^2 for the structure without imperfections. It seems that the load-bearing capacity of the structure, even if strongly reduced by the bad quality of the connection system, may be sufficient to meet the load demand of 40 kg/m^2 present on the 10th March 2010. Unfortunately the small application of imperfection with a 95th percentile of 3 millimetres is sufficient to drop the overall resistance from 53 to 45 kg/m^2.

It is expectable that at the moment of collapse several coercive states were acting on the structure, not only the non-planarity of supports, but also some assembly tolerances or some thermal differences that may have caused local overloads, not re-distributed because of the lack of ductility, that may have triggered a progressive collapse of the structure.

6.5 CONCLUSIONS

Figure 56 - collapsed truss system in Portomaggiore (FE)

In the previous chapter the steel truss system supporting roof of the gym in Portomaggiore (FE) has been analysed by means of both linear and non-linear analysis, calibrating some initial imperfection given by the supports differential settlements in order to understand if the vertical load-bearing capacity in this case may vary under different conditions od coercive states an ductility levels. In the following graph the maximum snow load that the truss system with the real connection resistances can bear as a function of initial imperfections.

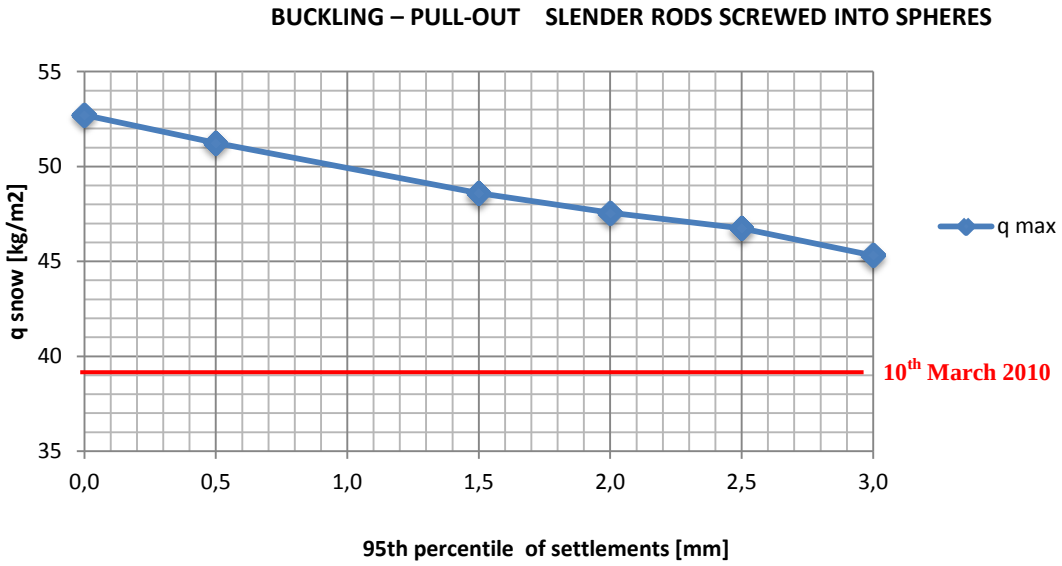

Figure 57 - ultimate snow load function of initial imperfections

In conclusion the main responsibility of the collapse, as reported from the engineers that investigated on this collapse, are to be addressed to the bad quality of the connection system composed of screwed spheres. By the way the load-bearing capacity of the truss system as a whole, even if decreased significantly, seems to be sufficient with respect to the snow load present at the moment of collapse. In fact the other drawback of the poor connection system is the brittleness of its pull-out failure mode, that together with the unavoidable presence of small coercive states given by the probable presence of imperfections such as supports settlements,

length tolerances or thermal actions, may have caused the activation of a progressive collapse of the structure. The collapse seems to be caused by the pull-out of some B82,5x5 rods, in the lower layer in central position and the consequent collapse of adjacent alignments until a full kinematism forms.

7. CONCLUSIONS

The aim of this thesis was to investigate the relation between coercive states that may be caused by imperfections such as differential settlements, thermal effects, and construction tolerances and the ultimate bearing capacity of static-indeterminate structures.

In particular the role of ductility has been analysed and in many cases it has been showed as a sufficient grade of ductility may lead to the insensibility of structures ultimate bearing capacity to imperfection and coercive states.

Both hand-made calculations, software based analysis and direct comparison of results have been employed to better understand the behaviour of different types of structures and materials, their related ductility and strength.

In conclusion ductility seems to play the major role in two positive benefits to the ultimate capacity of structures:

- ductility allows in general structures to develop a plastic collapse mechanism that leads to a larger load levels with respect to the first formation of local yielding;
- ductile structures bearing capacity showed a general independence from coercive states.

8. BIBLIOGRAPHY

1. P. Pozzati C. Ceccoli, *Teoria e tecnica delle strutture vol. 3 - Sistemi di travi - Interpretazione del collasso*; UTET; 1988;
2. K.E. Kurrer, *The history of the theory of structures*; Ernst&Sohn,2008;
3. Robert E. Melchers *Structural Reliability Analysis and Prediction;* Wiley, 1999;
4. Odone Belluzzi, *Scienza delle construzioni vol. 3 – La plasticità;* N. Zanichelli, 1960;
5. Alberto Carpinteri, *Structural Mechanics – a unified approach;* CRC Press, 1997;
6. Charles Massonet, Marcel Save, *Calcolo plastico a rottura delle Costruzioni;* Maggioli Editore 2008;
7. G. Ballio, C. Bernuzzi, *Progettare costruzioni in acciaio;* Hoepli, 2012;
8. G. Ballio, F.M. Mazzolani, *Strutture in acciaio;* ISEDI 1979;
9. a cura di P. Ruggeri, *Norme tecniche per le Costruzioni integrate con la Circolare applicativa;* EPC editore 2010;
10. T.H.G. Megson, *Structural and Stress analysis;* Butterworth Heinemann; 2005;
11. F. Leonhardt, E. Mönnig *C.A. & C.A.P. calcolo di progetto & tecniche costruttive*, ETS; 1976;
12. Baker et al., *The steel skeleton, Vol.2 : Plastic behaviour and design;* 1956;
13. S. Coccia, *Capacità rotazionale delle cerniere plastiche in C.A.*, 2007